4 Turbulent-flow modelling

This chapter provides an insight into the physical nature of turbulence and the mathematical framework that is used in numerical simulations of turbulent flows. The aim is to explain why turbulence must be modelled and how turbulence can be modelled, and also to explain what is modelled with different turbulence models. In addition, the limitations of the turbulence models are discussed. The intention is to give you such an understanding of turbulence modelling that you can actually suggest appropriate turbulence models for different kinds of turbulent flows depending upon their complexity and the required level of description.

4.1 The physics of fluid turbulence

Turbulence is encountered in most flows in nature and in industrial applications. Natural turbulent flows can be found in oceans, in rivers and in the atmosphere, whereas industrial turbulent flows can be found in heat exchangers, chemical reactors etc. Most flows encountered in industrial applications are turbulent, since turbulence significantly enhances heat- and mass-transfer rates. In industry a variety of turbulent multiphase flows can be encountered. Turbulence plays an important role in these types of flows since it affects processes such as break-up and coalescence of bubbles and drops, thereby controlling the interfacial area between the phases. Thus, turbulence modelling becomes one of the key elements in CFD.

In order to determine which turbulence-modelling approach is best suited to a particular application, we need to understand the limitations of various turbulence models. This insight requires a certain level of understanding of fluid turbulence. Probably everyone has an intuitive understanding of what turbulence is, since turbulence is encountered daily. From everyday experiences e.g. mixing coffee and milk, we know that turbulence increases the disorder in a fluid, resulting in an efficient mixing of fluid elements. As has already been mentioned, turbulence significantly affects mass-, momentum- and heat-transfer rates. High mass- and heat-transfer rates are positive and crucial aspects of many processes. In contrast, increased momentum transfer is usually undesirable, since it results in higher skin friction and hence drag. In other words, turbulence is an unavoidable feature of many chemical processes because high throughputs imply turbulent conditions. In this section we will take a closer look at what characterizes turbulence.

According to Hinze [5], turbulence can be characterized as follows:

Turbulent fluid motion is an irregular condition of flow in which the various quantities show random variation with time and space coordinates, so that statistically distinct average values can be discerned.

Indeed, turbulence is a state of fluid flow that can be characterized by random and chaotic motions. However, we need a deeper understanding of fluid turbulence before we can discuss turbulence modelling and understand the limitations of particular turbulence models.

4.1.1 Characteristic features of turbulent flows

Since it is difficult to give an exact definition of turbulence, we will look into several characteristic features of fluid turbulence. Observations of whirling smoke above a cigarette or other turbulent motions clearly show that large vortices in such motions are unstable and break up into smaller vortices. From such an observation it can also be seen that the flow becomes less chaotic far away from the cigarette. These two observations tell us that turbulence is a decaying process whereby large turbulent structures break up into subsequently smaller and smaller structures until the flow becomes laminar. Actually, turbulence dies out rather quickly if energy is not continuously supplied. There are more characteristic features of turbulence that can be identified by studying turbulent flows. Tennekes and Lumley [6] did not give a precise definition of turbulence; instead they listed the most important features of turbulence. These characteristic features are as follows.

(1) Irregularity. Turbulent flows are irregular, random and chaotic, and consist of a wide range of length scales, velocity scales and timescales. The large-scale motions in turbulent flows are usually referred to as large eddies or large vortices. A turbulent eddy is a turbulent motion that over a certain region is at least moderately coherent. The region occupied by a large turbulent eddy can also contain smaller turbulent eddies. This means that different scales coexist and smaller scales exist inside large scales. In turbulent flows the largest scales are bounded by the geometry of the flow, whereas the smallest scales are bounded by viscosity. The smallest eddies are generally several order of magnitudes smaller than large eddies. While eddies move they stretch, rotate and break up into two or more eddies. The irregularity of turbulent flows and the wide range of length scales and timescales make a deterministic approach to turbulence simulation very difficult. Statistical models are therefore frequently used in practical engineering simulations. An instantaneous representation of turbulent eddies in a pipe flow is shown in Figure 4.1.

Passages of large and small eddies through a certain point in a turbulent-flow field induce irregular velocity fluctuations. A point measurement of the instantaneous velocity in a turbulent flow yields a fluctuating velocity field similar to the one shown in Figure 4.2. Note that passages of large eddies through this point induce

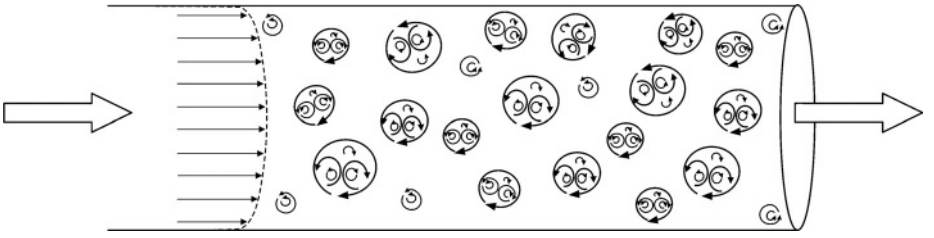

Figure 4.1 Large- and small-scale turbulent structures in a turbulent pipe flow.

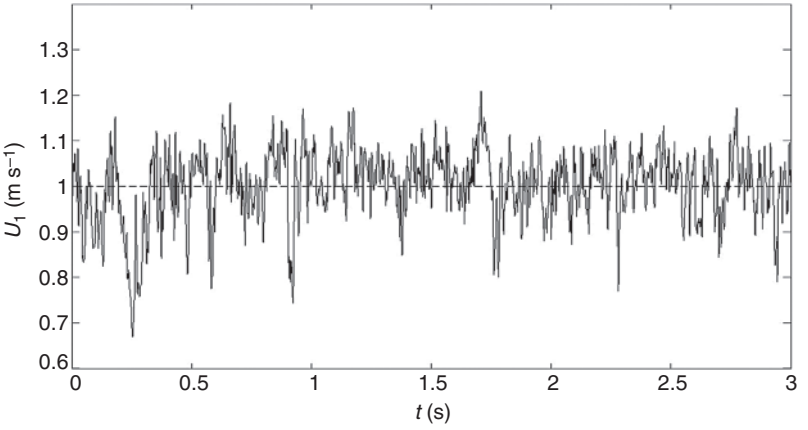

Figure 4.2 Instantaneous velocity at a certain point in a turbulent flow.

fluctuations of large amplitude and low frequency, whereas small eddies induce fluctuations of small amplitude and high frequency.

(2) Diffusivity. Probably the most important characteristic of turbulence is that it is diffusive. The turbulent diffusive transport is due to the chaotic motions in the flow and allows faster mixing rates of species, momentum and energy than would be allowed by the molecular diffusion alone. These rates are generally several orders of magnitude larger than the rate of molecular diffusion. Since turbulence is a 3D phenomenon, the turbulent transport occurs in all three dimensions. A simplified illustration of this turbulent transport is shown in Figure 4.3. In this figure two fluid elements are transported perpendicular to the streamlines. In contrast to laminar flow, this transport occurs even though the mean velocity component is zero in the y direction.

(3) Instability at large Reynolds numbers. Turbulence arises due to instabilities occurring at high Reynolds numbers. From a physical point of view this happens when the timescale for viscous damping of a velocity fluctuation is much larger than the timescale for convective transport. An extended discussion of this process is given in Section 4.1.3. From a mathematical point of view this can also be seen in the Navier–Stokes equation, where the nonlinear convective term becomes more important

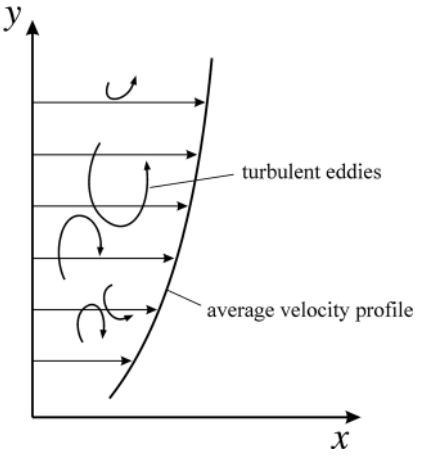

Figure 4.3 Transport due to turbulent convection.

than the viscous term with increasing Reynolds number. In dimensionless form the Navier–Stokes equation reads

$$\frac{\partial \widetilde{U_i}}{\partial \tilde{t}} + \widetilde{U_j}\frac{\partial \widetilde{U_i}}{\partial \tilde{x}_j} = -\frac{\partial \widetilde{P}}{\partial \tilde{x}_i} + \frac{1}{Re}\frac{\partial^2 \widetilde{U_i}}{\partial \tilde{x}_j\, \partial \tilde{x}_j}. \tag{4.1}$$

Thus the tendency towards instability, which is damped by viscosity, increases with the Reynolds number. Turbulent flows appear random in time and space, and are not experimentally reproducible in detail. Note that the nature of turbulence is random even though the Navier–Stokes equations are deterministic. In any turbulent flow there are unavoidable perturbations in initial conditions, boundary conditions and material properties. Turbulent fields display an acute sensitivity to such perturbations. This means that turbulence is stochastic even though the Navier–Stokes equations are deterministic.

(4) Three-dimensional structures. Turbulence is intrinsically 3D. The reason for this is that mechanisms such as vortex stretching and vortex tilting cannot occur in two dimensions (see the discussion in Section 4.1.6). Nevertheless, turbulent flows can be 2D in a statistical sense, hence 2D simulations of turbulent flows can be performed. Actually most turbulence modelling applied to practical engineering applications is based on models in which the 3D fluctuations are filtered out, thus not resolving the turbulent fluctuations, but do resolve the coupling between the fluctuations and the mean flow field.

(5) Dissipation of turbulent kinetic energy. In all turbulent flows there is a flux of energy from the largest turbulent scales to the small scales. At the smallest scales the turbulent kinetic energy is dissipated into heat due to viscous stresses. This flux of energy is commonly referred to as the energy cascade. The idea of the energy cascade is that kinetic energy enters the turbulence at the largest scales at which energy is extracted from the mean flow. By inviscid processes this energy is then transferred to smaller and smaller scales. The reason for this energy flux is that large eddies are

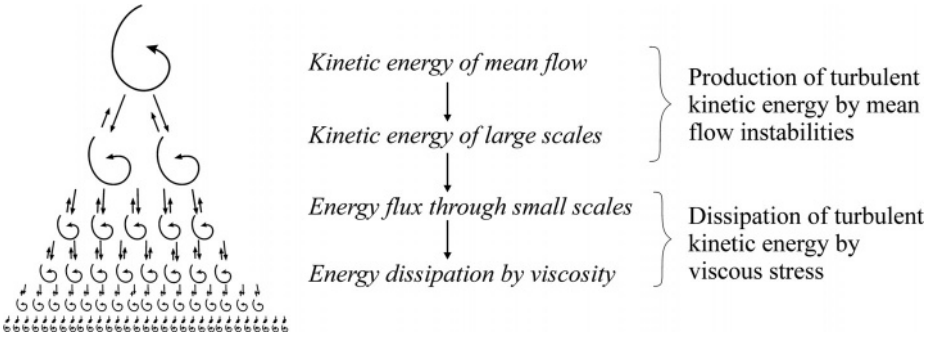

Figure 4.4 Energy flux from large to small scales.

unstable and break up into smaller eddies, thereby transferring the energy to smaller scales. These smaller eddies undergo similar break-up processes and transfer the energy to yet smaller eddies. On the smallest scale we find the dissipative eddies, whose energy is dissipated into heat by viscous action due to molecular viscosity. This energy flux is illustrated in Figure 4.4. A consequence of the dissipation is that turbulence decays rapidly if no energy is supplied to the system. In chemical processes energy is supplied to systems in numerous ways. In a turbulent pipe flow, the energy is supplied by the pump, whereas in a stirred-tank reactor the energy is supplied by the impeller. The amount of energy supplied to these systems can be determined from the pressure drop and torque, respectively. It should be pointed out that the total energy input equals the sum of energy losses due to energy dissipation in the fluid and at the walls.

(6) Continuum. Turbulence is a continuum phenomenon in which even the smallest scales of turbulence are much larger than the molecular length scale. The motion of fluids is therefore described by the conservation equations for mass and momentum conservation supplemented by initial and boundary conditions.

(7) Turbulent flows are flows. Turbulence is a feature of a flow, not a fluid. This means that all fluids can be turbulent at high enough Reynolds number.

4.1.2 Statistical methods

More than a century ago, Reynolds introduced statistical averaging methods for turbulent flows. Statistical methods still remain crucial in the theory of turbulence and in turbulence modelling. These methods are used to study mean values of flow properties in space and time. By using statistical methods, the need for information about the flow is reduced and the flow description is considerably simplified. In this book we will focus on single-point statistics. Even though one-point quantities do not encompass the full statistics of the flow, they still include many of the more important measures of turbulent flows such as the mean flow velocity, $\langle U_i \rangle$, and the turbulent kinetic energy per unit mass, $\langle u_i u_i \rangle / 2$. Spectral analysis is an example of another method that better describes the flow. With this method, it is even possible to capture the contributions of different scales to the

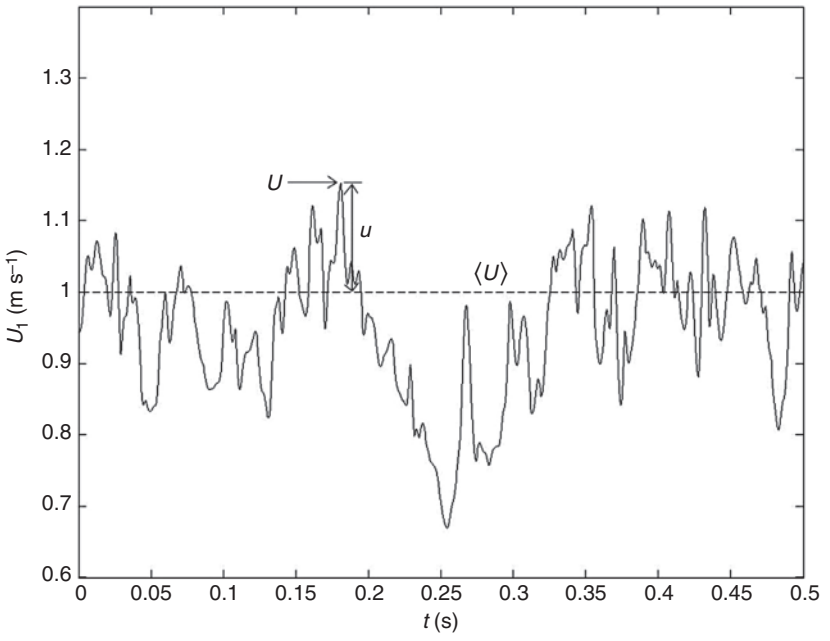

Figure 4.5 Velocity decomposition of instantaneous velocity.

overall energetics of turbulence. For more information about spectral analysis and other advanced methods the reader is referred to textbooks on turbulence [7–12].

One-point measurement of the instantaneous velocity reveals that passage of small eddies induces fluctuations of small amplitude and high frequency, whereas passage of large eddies induces fluctuations of large amplitude and low frequency. Frequencies ranging from 1 Hz to 10 000 Hz are commonly observed in air and water flows. An example of such a measurement is shown in Figure 4.5. In this figure it can be seen that fluctuations with different frequencies exist. In the one-point statistics, the instantaneous velocity at any particular position and time, $U_i(x, t)$, is divided into an average and a fluctuating part. The average represents the mean velocity, whereas the fluctuating parts is usually interpreted as representing the turbulence. Decomposition of the instantaneous velocity into its mean and fluctuating parts is then represented as

$$U_i = \langle U_i \rangle + u_i, \tag{4.2}$$

where the average velocity is defined as

$$\langle U_i \rangle = \frac{1}{2T} \int_{-T}^{T} U_i \, dt. \tag{4.3}$$

The timescale used in this filtering operation is chosen so that the instantaneous variables are averaged over a time period that is large compared with the turbulent timescales but small compared with the timescale of the mean components. Thus, turbulent flows can be considered to consist of randomly varying components superimposed on a mean

motion. This decomposition is known as Reynolds decomposition since Reynolds first introduced the concept in the analysis of turbulent flows. The intensities of velocity fluctuation in different directions can be measured in terms of the turbulent kinetic energy per unit mass

$$k = \frac{1}{2}\langle u_i u_i \rangle = \frac{1}{2}\sum_{i=1}^{3}\langle u_i^2 \rangle = \frac{1}{2}\left(\langle u_1^2 \rangle + \langle u_2^2 \rangle + \langle u_3^2 \rangle\right). \tag{4.4}$$

Let us now define what we mean by turbulent kinetic energy. The kinetic energy of the fluid (per unit mass) at a specific point in time is given by

$$E = \frac{1}{2}U_i U_i. \tag{4.5}$$

The mean of the kinetic energy can be decomposed into two parts,

$$\begin{aligned}\langle E \rangle &= \frac{1}{2}\langle (\langle U_i \rangle + u_i)(\langle U_i \rangle + u_i) \rangle = \frac{1}{2}(\langle U_i \rangle \langle U_i \rangle + \langle u_i u_i \rangle) \\ &= \frac{1}{2}\langle U_i \rangle \langle U_i \rangle + k = \overline{E} + k,\end{aligned} \tag{4.6}$$

where $\overline{E}$ is the kinetic energy of the mean flow and k is the turbulent kinetic energy per unit mass, $\frac{1}{2}\langle u_i u_i \rangle$.

To solve the Navier–Stokes equations, the pressure is decomposed in a similar way:

$$P = \langle P \rangle + p. \tag{4.7}$$

For incompressible fluids there is no need for decomposition of any other quantities than velocity and pressure. However, for compressible fluids the density must also be decomposed.

Definition of various statistical symmetries

A steady or stationary turbulent flow is defined as one whose statistical properties do not change with time. Homogeneity implies that, given any number of different spatial points and times, the statistics will remain unchanged if all positions are shifted by the same constant displacement. In other words, the statistics of the flow are invariant under translation. If the statistics are also invariant under rotation and reflection, the flow is isotropic. Isotropy is therefore a stricter criterion than homogeneity. Assumptions of homogeneous and isotropic turbulence are often made in theoretical studies, since these assumptions simplify equations and analysis. We can summarize the statistical symmetries as

- statistically stationary, if all statistics are invariant under a shift in time;
- statistically homogeneous, if all statistics are invariant under a shift in position (translation);
- statistically isotropic, if all statistics are invariant under rotations and reflections.

Even though homogeneous turbulence is rarely encountered in practice it is still possible to produce laboratory flows close to homogeneity. Grid-generated turbulence is an example of approximately homogeneous turbulence. These flows are homogeneous in

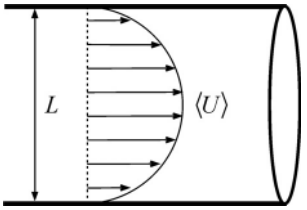

Figure 4.6 Pipe flow.

the sense that the variations of the statistical properties take place over distances large compared with the length scales of the turbulence itself. Grid turbulence in wind tunnels is therefore extensively studied in academia. Knowledge originating from experiments of this type has been widely used to develop and validate turbulence models.

4.1.3 Flow stability

Recall that the Reynolds number is often used to determine the transition between laminar and turbulent flows. The Reynolds number is the ratio of inertial force to viscous force,

$$Re = \frac{\langle U \rangle L}{\nu}. \tag{4.8}$$

Hence, increasing the Reynolds number represents a relative increase in the inertial force in relation to the viscous force. Transition from laminar to turbulent flow is related to the presence of a disturbance and its amplification. Thus the damping or amplification of a small velocity fluctuation in laminar flow determines the stability of the flow. If the disturbance is damped, the flow remains stable and laminar. On the other hand, if it is amplified, the flow becomes unstable and this can lead to turbulence through transition. Transition from laminar to turbulent flow occurs when the time taken to equilibrate with a wall due to diffusive transport is much larger than the time for convective transport. Consider a pipe flow, illustrated in Figure 4.6, characterized by a pipe diameter L, an average velocity $\langle U \rangle$ and a velocity fluctuation u.

Turbulent eddies are created in the near-wall region and, when there is a lack of damping by viscosity, they can move across the pipe, keeping the flow turbulent. If u is the eddy velocity and L is proportional to the nearest surface that can damp the turbulent fluctuations, the necessary time for this transport is

$$t_c = L/u. \tag{4.9}$$

During this time period viscosity acts on a distance

$$l = (t_c \nu)^{1/2}. \tag{4.10}$$

This means that viscosity is able to damp velocity fluctuations of scale smaller than l. The condition for turbulent flow is then given by

$$l < L, \tag{4.11}$$

or

$$l = (t_c \nu)^{1/2} < L. \tag{4.12}$$

Substitution of Eq. (4.9) into Eq. (4.12) leads to the condition

$$\frac{uL}{\nu} \gg 1. \tag{4.13}$$

Note that the velocity fluctuations, u, are usually much smaller than the average velocity in the pipe, $\langle U \rangle$. Thus, the criterion for turbulent flow in pipes in terms of the average velocity is given by

$$Re = \frac{\langle U \rangle L}{\nu} \gg 1. \tag{4.14}$$

This means that, for high-Reynolds-number flows, $Re \gg 1$, viscosity cannot damp velocity fluctuations and the flow becomes turbulent. The first systematic studies regarding the transition to turbulence were carried out by Osborne Reynolds more than a century ago. Reynolds studied flow in glass tubes and obtained a critical Reynolds number 2100 at which the flow ceased to be laminar. By eliminating disturbances at the inlet of the tube, it has been possible to maintain laminar flow even for Reynolds numbers one order of magnitude larger than that.

Experimental studies have shown that the following Reynolds-number criteria can be used to predict the transition from laminar to turbulent flow.

(1) For internal flows,
   - pipe flow, $Re > 2100$;
   - flow between parallel plates, $Re > 800$.

(2) For external flows,
   - flow around a sphere, $Re > 350$.

(3) Boundary layers,
   - flow along surfaces, $Re > 500\,000$.

Note that different characteristic lengths are used in the definitions of the Reynolds numbers above. It should also be noted that surface roughness affects the transition as well.

4.1.4 The Kolmogorov hypotheses

In 1941, Kolmogorov stated three prominent hypotheses that are of fundamental importance for the understanding of turbulence. The first hypothesis concerns the isotropy of small-scale turbulent motions. Kolmogorov argued that there are reasons to expect that at high Reynolds number the directional information is lost in the chaotic scale-reduction process. Whereas the anisotropic large-scale structures, l_0, depend on geometry and boundary conditions, it is assumed that the small scales have small timescales and that these motions are statistically independent of the large-scale turbulence and of the mean flow. In other words, somewhere in the process whereby turbulent eddies are reduced in

size all directional information is lost. On this scale turbulence is statistically isotropic and these scales are therefore independent of the geometry.

Kolmogorov's hypothesis of local isotropy:

At sufficiently high Reynolds numbers, the small scales of turbulent motions, $l \ll l_0$, are statistically isotropic.

Kolmogorov also argued that the statistics of small-scale motions are universal, i.e. similar in every high-Reynolds-number flow. This argument forms the basis for the second hypothesis. For the small-scale motions, the isotropic scales ($l < l_{\mathrm{EI}}$), the transfer of energy to successively smaller scales and energy dissipation are the dominant processes. This leads to the conclusion that the energy-transfer rate and the kinematic viscosity are the two important parameters determining the statistics of the small-scale motions. In other words, turbulent structures much smaller than the anisotropic structures are universal, being solely determined by the energy-dissipation rate, ε, and the viscosity, ν. This hypothesis is known as 'Kolmogorov's first similarity hypothesis'.

Kolmogorov's first similarity hypothesis (dissipative range):

In every turbulent flow at sufficiently high Reynolds number, the statistics of the small-scale motions, $l < l_{\mathrm{EI}}$, have a universal form that is uniquely determined by viscosity, ν, and dissipation rate, ε.

The characteristic length scale, velocity scale and timescale in the dissipative range are thus given by the energy-dissipation rate, ε, and the viscosity, ν. These scales are also known as the Kolmogorov scales. The Kolmogorov scale, η, characterizing the size of the smallest turbulent eddies, which is the scale for dissipation of turbulent kinetic energy, is

$$\eta = \left(\frac{\nu^3}{\varepsilon}\right)^{1/4} \tag{4.15}$$

and the Kolmogorov velocity scale is given by

$$u_\eta = (\varepsilon \nu)^{1/4}. \tag{4.16}$$

The Kolmogorov timescale, τ_η, for viscous dissipation is given by

$$\tau_\eta = \left(\frac{\nu}{\varepsilon}\right)^{1/2}. \tag{4.17}$$

By definition Kolmogorov's length and velocity scales give a Reynolds number equal to 1. Thus, the smallest-scale motion of turbulence is laminar, being solely determined by viscous forces.

Within the range $l < l_{\mathrm{EI}}$ the timescales are small compared with the timescales for the large eddies. This means that the small eddies can adapt quickly to maintain a dynamic equilibrium with the energy-transfer rate imposed by the large eddies. Since the statistics of the small-scale motions are universal, this range $l < l_{\mathrm{EI}}$ is often referred to as the universal equilibrium range.

Kolmogorov also stated a 'second similarity hypothesis' in which it is assumed that for a special range of structures within the universal equilibrium range viscosity plays

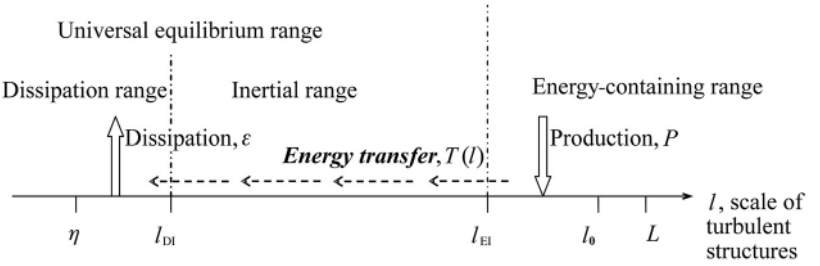

Figure 4.7 The cascade of turbulence energy on a logarithmic scale.

a negligible role in the motions. This means that only the energy-dissipation rate, ε, determines the statistics of the motions in this range. This is the so-called inertial range.

Kolmogorov's second similarity hypothesis (inertial range):

In every turbulent flow at sufficiently high Reynolds number, the statistics of the motions of scale l in the range $\eta \ll l \ll l_0$ have a universal form that is uniquely determined by ε and independent of ν.

On introducing a length scale $l_{\mathrm{DI}} = 60\eta$, the inertial range is given by $l_{\mathrm{DI}} < l < l_{\mathrm{EI}}$. Note that the length scale l_{DI} splits the universal equilibrium range into two subranges. These subranges are the inertial range, $l_{\mathrm{DI}} < l < l_{\mathrm{EI}}$, and the dissipative range, $l < l_{\mathrm{DI}}$.

Thus, according to the two similarity hypotheses, the motions in the inertial subrange are determined solely by inertial effects, whereas the motions in the dissipation range experience significant viscous effects. Figure 4.7 shows the various length scales and ranges.

4.1.5 The energy cascade

The basic idea in the energy-cascade theory, illustrated in Figure 4.7, is that there is a net flux of energy from large to small eddies. The idea of energy transfer from large to subsequently smaller scales was introduced by Richardson in 1922. In the energy cascade there is a source of turbulent energy, P, at the largest scales. On the largest scales energy is extracted from the mean flow instabilities. This means that, if there were no flow, no fluctuations would be sustained; hence the mean flow drives the fluctuations. Thus, the energy cascades start with energy transfer from the mean flow to the largest eddies. It is assumed that large eddies contain the largest part of the energy and contribute little to the energy dissipation. It is also assumed that the largest eddies in turbulent flows do most of the transport of momentum and other quantities. Since the continuous supply of energy can neither accumulate in large eddies nor just disappear, there must be a sink of energy. The sink of energy is twofold. Energy is finally transferred to heat on the bounding surfaces and it goes into heating up the fluid itself. Actually, the energy-cascade theory explains the latter mechanism. It is assumed that the flux of energy continues to successively smaller scales until the viscous stress becomes effective. On this scale, turbulent kinetic energy is dissipated as heat by molecular viscosity. The

Table 4.1 Correlations for various turbulence scales

Scale	Length	Time	Velocity
Large scale	$l = k^{3/2}/\varepsilon$	$\tau_l = k/\varepsilon$	$u_l = \left(\frac{2}{3}k\right)^{1/2}$
Smallest scale	$\eta = (\nu^3/\varepsilon)^{1/4}$	$\tau_\eta = (\nu/\varepsilon)^{1/2}$	$u_\eta = (\varepsilon\nu)^{1/4}$

energy-dissipation process is a result of viscous friction between layers of fluid moving at different velocities. An important consequence of the viscous stress is that it prevents the generation of infinitely small eddies. Hence, in all fluid flows there is a minimum scale of turbulent structures.

Discussions of the energy cascade often refer to the universal equilibrium range. This terminology is based on the argument that the small eddies will evolve much more rapidly than the large eddies. Thus eddies in the universal range can adjust so quickly to changes in external conditions that they can be assumed to be always in a state of local equilibrium. The transfer of energy in the cascade is given by

$$T_{\mathrm{EI}} = T(l_{\mathrm{EI}}) = T(l) = T_{\mathrm{DI}} = T(l_{\mathrm{DI}}) = \varepsilon. \tag{4.18}$$

In conclusion, the energy-cascade theory places production at the beginning and dissipation at the end of a sequence of processes. L and l_0 in Figure 4.7 are the flow scale and the scale of the largest eddies, respectively. The length scale l_0 is a measure of the largest turbulent eddies, which contain most of the turbulent kinetic energy. l_0 is given by

$$l_0 = \frac{k^{3/2}}{\varepsilon}. \tag{4.19}$$

The characteristic timescale for the large eddies, τ_l, is the time necessary to decrease a turbulent structure of size l_0, that is the 'eddy lifetime'. This timescale can also be seen as the timescale for transfer of turbulent kinetic energy from the scale l_0 to η, which means that it is a measure for the turbulence decay rate. τ_l is given by

$$\tau_l = \frac{k}{\varepsilon}. \tag{4.20}$$

Since k is defined as $\frac{1}{2}\left(u_1^2 + u_2^2 + u_3^2\right)$, the characteristic velocity scale for the large eddies is given by

$$u_l = \left(\frac{2}{3}k\right)^{1/2}. \tag{4.21}$$

As a rule of thumb, l_{EI} can be used as a demarcation between anisotropic and isotropic turbulent eddies, see Figure 4.7. The length scale of the anisotropic large eddies is then given by $l > l_{\mathrm{EI}}$ and that for isotropic eddies by $l < l_{\mathrm{EI}}$. This demarcation requires an approximation of l_{EI}, which is given by $l_{\mathrm{EI}} \approx \frac{1}{6}\, l_0$. The relations for the various scales of turbulent motions are summarized in Table 4.1.

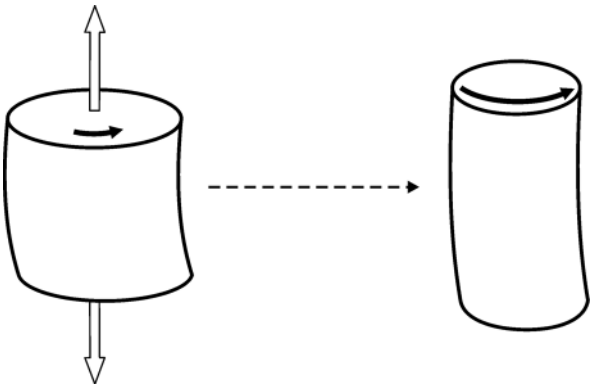

Figure 4.8 Stretching of a vortex tube concentrates vorticity on progressively smaller scales.

From the correlations in Table 4.1 we can determine the smallest turbulent scales (Kolmogorov scales) in a 100-W kitchen mixer. Assume that the mixer is filled with 1 litre of water ($\nu = 10^{-6}\ \mathrm{m^2\,s^{-1}}$ and $\rho = 10^3\ \mathrm{kg\,m^{-3}}$) and that all energy put into the system is dissipated homogeneously in the fluid. Since $\mathrm{W} = \mathrm{J\,s^{-1}} = \mathrm{m^2\,kg\,s^{-3}}$, the energy-dissipation rate per unit mass, ε, is equal to $100\ \mathrm{m^2\,s^{-3}}$. Hence, the smallest turbulent length scale in the mixer is $\eta = (\nu^3/\varepsilon)^{1/4} = 10\,\mu\mathrm{m}$ and the characteristic timescale for these eddies is $\tau_\eta = (\nu/\varepsilon)^{1/2} = 0.1\,\mathrm{ms}$.

4.1.6 Sources of turbulence

Turbulent flows require a continuous supply of energy since turbulence is inherently dissipative. In the energy-cascade theory the source of energy enters at the largest scale, at which energy is extracted from the mean flow by the large-scale eddies. Whereas large eddies extract energy from the mean flow, small eddies are supplied with energy from the flux of energy from the large eddies. This energy transfer between eddies is assumed to be related to vortex stretching and the conservation of angular momentum when eddies are stretched. The interaction between vorticity and velocity gradients is an important mechanism to create and maintain turbulence. Two idealized mechanisms that result from this interaction are vortex stretching and vortex tilting. On average these mechanisms create smaller and smaller scales. Hence, stretching and tilting of vortices create and maintain turbulence at smaller scales. The stretching mechanism is illustrated in Figure 4.8. Stretching of a vortex tube means that the cross-section of the vortex tube decreases in size (for an incompressible fluid). In other words, the size of the vortex, as estimated from its transverse dimensions, becomes smaller. This argument shows how larger vortices or eddies in a turbulent fluid can give rise to smaller ones. The stretching work done by the mean flow on large eddies provides the energy which maintains turbulence. Smaller eddies are themselves stretched by somewhat larger eddies. In this way, energy transfers to progressively smaller scales. In this process the orientation of large eddies imposed by the mean flow is lost. Thus small scales will be

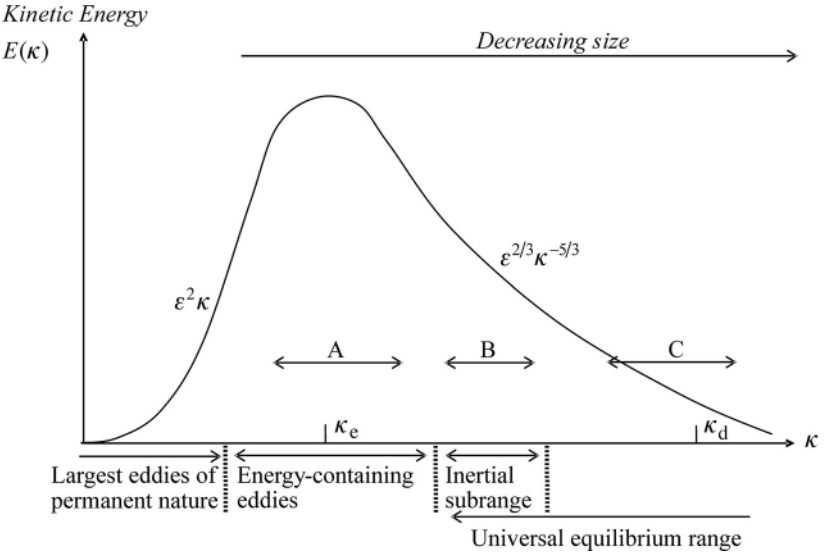

Figure 4.9 Turbulent kinetic energy spectrum.

isotropic. Turbulent flows dissipate energy as the viscous stresses act on the smallest scales. On this scale energy is dissipated into heat due to molecular viscosity.

4.1.7 The turbulent energy spectrum

At high Reynolds numbers, turbulent flows are characterized by the existence of a wide range of length scales that are bounded from above by the dimensions of the flow field and bounded from below by the diffusive action of molecular viscosity. One important tool for analysing the different regions of turbulence is the energy spectrum. It is common practice to use wave numbers instead of length scales. The dimension of a wave number is one over length, thus we can think of the wave number as inversely proportional to the eddy radius, i.e. $\kappa \propto 1/r$. This means that large wave numbers correspond to small eddies and small wave numbers to large eddies. Eddies with wave numbers in the region of κ_e, Figure 4.9, contain the largest part of the energy and contribute little to the energy dissipation. However, the small eddies, which are of very high frequency, in the region of κ_d, dissipate energy. Here, turbulent kinetic energy is dissipated into heat by molecular viscosity. The viscous stresses prevent the generation of eddies with higher frequency. In wave-number space, the energy of eddies from κ to $\kappa + d\kappa$ can be expressed as

$$E(\kappa)d\kappa. \tag{4.22}$$

The total turbulent kinetic energy, k, which is the sum of the kinetic energies of the three fluctuating velocity components, i.e. $k = \frac{1}{2}\langle u_i u_j \rangle$, is obtained by integrating over the whole wave-number space

$$k = \int_0^\infty E(\kappa)d\kappa. \tag{4.23}$$

The energy spectrum of fully developed homogeneous turbulence is thought to be composed of three distinct wave-number regions (see Figure 4.9).

A. In this region the large energy-containing eddies are found. These eddies interact with the mean flow and extract energy from the mean flow. The energy is transferred to slightly smaller scales and eventually into region B.
B. This region is the inertial subrange. In this region turbulent kinetic energy is neither produced nor dissipated. However, there is a net flux of energy through this region from A to C. The existence of this region requires that the Reynolds number is high.
C. This is the dissipative region where turbulent kinetic energy is dissipated into heat. Eddies in this region are isotropic and the scales are given by the Kolmogorov scales.

A spectral analysis of the turbulence scales often reveals a region where the distribution obeys the following relationship:

$$E(\kappa) = C_\kappa \varepsilon^{2/3} \kappa^{-5/3}, \qquad \frac{1}{l_0} \ll \kappa \ll \frac{1}{\eta}. \tag{4.24}$$

This equation is called the Kolmogorov spectrum law, or simply the $-5/3$ law. The equation states that, if the flow is fully turbulent, the energy spectra should exhibit a $-5/3$ decay. The region where this law applies is known as the inertial subrange and is the region where the energy cascade proceeds in local equilibrium. This law is often used in experiments and simulations (DNS, LES) to verify that the flow is fully turbulent. Note that the largest eddies, κ_e, contain most of the turbulence energy and are therefore responsible for most of the turbulent transport. Nevertheless, the small eddies are responsible for mixing on the small scales.

Questions

(1) Describe the process of transition from laminar to turbulent flow.
(2) Discuss how turbulence can be characterized.
(3) Explain the source of the energy supplied to eddies, why eddies have a lower limit in size and why the turbulent velocity field is isotropic within that range.
(4) Explain what is meant by the energy-containing range, the inertial subrange and the dissipative range in the energy spectrum.
(5) Explain what is meant by vortex stretching and relate it to the energy cascade through the eddy sizes.

4.2 Turbulence modelling

Turbulence modelling ranges from weather forecasts to virtual prototyping of novel cars, airplanes, heat exchangers, gas-turbine engines, chemical reactors etc. Accurate simulations of turbulent flows are therefore of high interest both for society and in industry. Hence, turbulence modelling is one of the key elements in CFD. This section

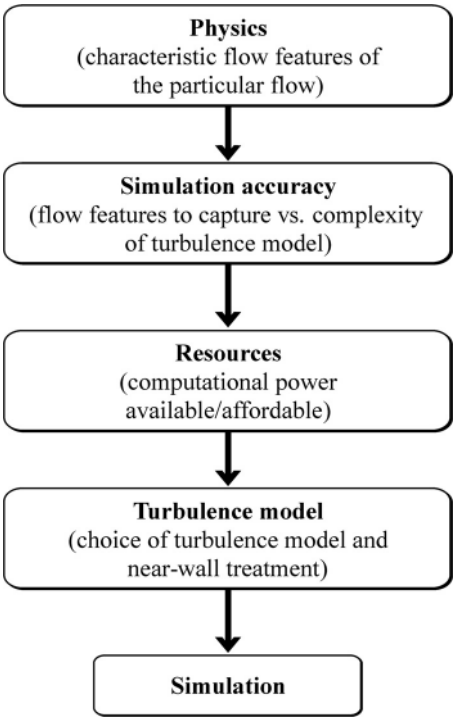

Figure 4.10 Schematic characterization of the modelling process.

will discuss some of the numerous approaches to modelling turbulent flows that have been suggested in the literature.

Unfortunately turbulent flows are characterized by fluctuating velocity fields in which there exist small-scale and high-frequency fluctuations. Thus an enormous amount of information is required if one is to describe turbulent flows completely. High-Reynolds-number flows are therefore too computationally expensive to simulate in detail. Fortunately, we usually require something less than the complete time history of every flow property over all spatial coordinates. Instead of simulating the exact governing equations, these equations can be manipulated to remove the small-scale high-frequency fluctuations, resulting in a modified set of equations that it is computationally less expensive to solve. As a consequence of the manipulation, the modified equations contain additional unknown variables. Hence, turbulence models are needed in order to determine these variables. Turbulence modelling can therefore be described as the process of closing the modified Navier–Stokes equations by providing required turbulence models.

During the last few decades numerous turbulence models of varying complexity have been proposed. The selection among these models is crucial for a successful simulation. In the ideal case the selection process will be a straightforward procedure as shown in Figure 4.10. As indicated in Figure 4.10, knowledge about the flow (i.e. whether or not the flow involves separation, whether the features of the flow result from anisotropy etc.) significantly simplifies the decision by reducing the number of turbulence models

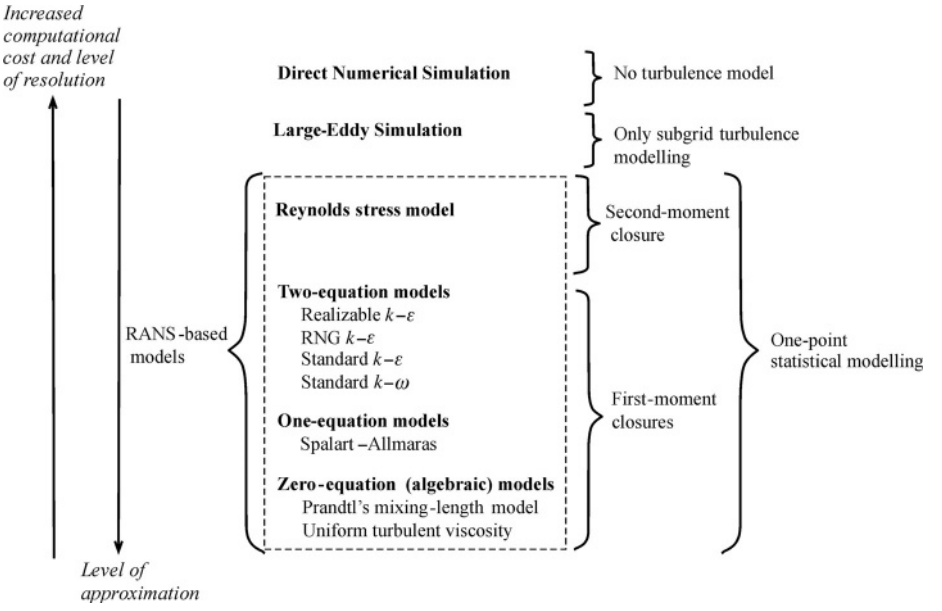

Figure 4.11 A schematic overview of turbulence modelling.

that can be used. Furthermore, in practical engineering applications the selection of turbulence models can be restricted by the computational resources that are available or affordable. It is not always the case that the required simulation accuracy implies the use of a turbulence model that can be matched with the available computational power.

In this section we give an overview of the most commonly used turbulence models and their limitations. Be forewarned that no models exist for general purposes and that every model must be used with care. A general trend for the turbulence models is that the fewer approximations are introduced, the more computational power is required. Figure 4.11 gives an overview of the different turbulence models discussed in this section. As is clearly illustrated in the figure, there is a trade-off between model accuracy and computational cost.

The choice among the models presented in Figure 4.11 is crucial for successful simulations. For simple flows good predictions can be obtained with simple turbulence models such as one-equation models. Even though the result may be less accurate for complex flows, such models may still allow one to screen effects of various design changes early in a project. The quality of the simulations is then reduced to obtaining information about trends rather than obtaining an overall accurate prediction. With the rapid development of computers and CFD codes it is expected that routine simulations will incorporate increasingly more advanced turbulence models in the future. Nevertheless, during the next few decades simulations of engineering applications will be based on turbulence models with various levels of approximation.

4.2.1 Direct numerical simulation

Direct numerical simulation (DNS) of turbulent flows may at first glance seem to be the most obvious and straightforward approach with which to simulate turbulent flows. Using DNS, in which the unsteady 3D Navier–Stokes equations are solved directly, there is no need for a turbulence model since the equations correctly describe fluid flows both for laminar and for turbulent conditions. The difficulty is actually solving these equations at high Reynolds number. Recall that a wide range of length scales and timescales exists in high-Reynolds-number turbulent flows. This means that all these turbulent scales must be resolved in the simulations. The scale of resolution needed is roughly described by the Kolmogorov length scale and timescale. Hence, very dense computational grids and short time steps are required. Add also that the equations are nonlinear and it is clear that this will challenge the computational solution algorithms, thus making any simulation very time-consuming. In fact, it will not be possible to perform DNS for real engineering problems until many more generations of computers have come and gone. Even if it were possible to perform these simulations for practical engineering applications, the amount of data would be overwhelming. At the present time DNS is a research tool rather than an aid to engineering design. The computational cost of DNS is high and it increases as the cube of the Reynolds number. For the interested reader, it can be mentioned that the computational cost for DNS of reactive flows is given by

$$t \propto Re^3 Sc^2. \tag{4.25}$$

Note that for gases $Sc \sim 1$, for liquids like water $Sc \sim 10^3$ and for very viscous liquids $Sc \sim 10^6$. DNS is thus mainly used for gaseous flows at moderate Reynolds numbers due to the high computational cost. Such deterministic simulations are useful for developing closures for statistical turbulence models and for validation of these models, but in practical engineering simulations DNS is less useful. Since DNS is of no use for practical engineering flow simulations, it will not be discussed further in this chapter.

4.2.2 Large-eddy simulation

Since the main problem in simulating high-Reynolds-number flows is the presence of very small length scales and timescales, a logical solution is to filter the equations, thus resolving only intermediate-to-large turbulence scales. Large-eddy simulation (LES) extends the usefulness of DNS for practical engineering applications by intentionally leaving the smallest turbulence scales unresolved. In LES the dynamics of the large scales are computed explicitly. Therefore, LES needs to be 3D and transient. The advantages of LES arise from the fact that the large eddies, which are hard to model in a universal way since they are anisotropic, are simulated directly. In contrast, small eddies are more easily modelled since they are closer to isotropy and adapt quickly to maintain a dynamic equilibrium with the energy-transfer rate imposed by the large eddies. The effects of the non-resolved scales, which cannot be neglected, are accounted for with subgrid stress models. This means that the subgrid models should be universal. In LES the turbulence

scales are usually resolved down to the inertial subrange, Figure 4.9. As a general rule of thumb at least 80% of the turbulence energy should be resolved in the calculated velocities. Substantial savings in computational cost are realized in LES, since a coarser grid is employed than that required for DNS, Figure 4.11. This allows modelling of flows at higher Reynolds number. Nevertheless, the computational cost for LES is high in comparison with those of other turbulence models. The high computational cost stems from a very fine grid, short time steps and long computational time taken to obtain reliable statistics.

Filtering of the Navier–Stokes equations

The governing equations for LES are obtained by spatially filtering over small scales. A generalized filter can be defined by

$$\overline{U_i}(x,t) = \iiint G(x-\xi;\,\Delta)U_i(\xi,t)\mathrm{d}^3\xi, \tag{4.26}$$

where the filter function is interpreted as acting to keep values of U_i occurring on scales larger than the filter width Δ. Basically the filter function, G, is some function that is effectively zero for values of U_i occurring at the small scales. Thus, filtering eliminates eddies whose scales are smaller than the filter width. Examples of such filters are the box, Gaussian and sharp spectral filters etc. [11]. By filtering the Navier–Stokes equations, the scales which will be modelled are separated from those which will be calculated directly.

The velocity field has the decomposition,

$$U_i(x,t) = \overline{U_i}(x,t) + u_i(x,t). \tag{4.27}$$

An important difference between this decomposition and the Reynolds decomposition, which is widely used in turbulence modelling, is that $\overline{U_i}$ is a random field and that in general the filtered residual is not zero,

$$\overline{u_i}(x,t) \neq 0. \tag{4.28}$$

The filtered continuity equation is

$$\frac{\partial \overline{U_j}}{\partial x_j} = 0 \tag{4.29}$$

and the filtered momentum equation is

$$\frac{\partial \overline{U}_i}{\partial t} + \frac{\partial \overline{U}_i\overline{U}_j}{\partial x_j} = -\frac{1}{\rho}\frac{\partial \overline{P}}{\partial x_j} + \nu\frac{\partial^2 \overline{U}_i}{\partial x_j\,\partial x_j} - \frac{\partial \tau_{ij}}{\partial x_j}. \tag{4.30}$$

The closure problem in LES arises from the residual stress tensor, τ_{ij}, which is also commonly referred to as the subgrid stress tensor. Here the term τ_{ij} describes the transfer of momentum by turbulence at scales that are smaller than the filter,

$$\tau_{ij} = \overline{U_iU_j} - \overline{U}_i\overline{U}_j. \tag{4.31}$$

The filtered velocities $\overline{U}_i$ and $\overline{U}_j$ are solved for but the correlation $\overline{U_iU_j}$ is unknown and a satisfactory subgrid stress model must be provided for τ_{ij}. The simplest models

usually involve modelling of a subgrid viscosity. An important difference between the subgrid viscosity and the traditional eddy viscosity is that it acts as a correction to the behaviour of the small scales, not as a correction of the entire influence of turbulence on the mean flow. This means that the subgrid viscosity is small compared with the eddy viscosity used in the eddy-viscosity models.

One frequently used model is the Smagorinsky–Lilly model. In this model the isotropic stress is included in the modified filtered pressure

$$\tilde{p} = \overline{p} + \frac{2}{3}\tau_{ii} \tag{4.32}$$

and the anisotropic part is modelled using a linear eddy-viscosity model,

$$\tau_{ij} - \tfrac{1}{3}\tau_{kk}\delta_{ij} = -2\mu_t \overline{S}_{ij}. \tag{4.33}$$

The subgrid viscosity is then calculated from

$$\mu_{\mathrm{t}} = \rho L_S^2 \left|\overline{S}\right|, \tag{4.34}$$

where

$$\left|\overline{S}\right| = \sqrt{2\overline{S}_{ij}\overline{S}_{ij}} \qquad \text{and} \qquad L_S = \min(\kappa d, C_{\mathrm{S}} V^{1/3}), \tag{4.35}$$

κ is the von Kármán constant, d is the distance to the nearest wall and V is the volume of the computational cell. The Smagorinsky coefficient C_{S} is of the order of 0.17 but depends, unfortunately, on the flow conditions and grid size. The interested reader is referred to [7, 11] for more information about LES. More advanced LES models, e.g. dynamic LES, also estimate the Smagorinsky coefficient by filtering on two different scales.

4.2.3 Reynolds decomposition

Industrial applications of LES are expected to increase in the near future. However, like DNS, LES is currently too computationally expensive for routine simulations. In many cases the industrial and academic communities need even simpler models than LES. In this chapter we introduce turbulence models that are widely used for simulations of engineering applications. These models are based on a method by which the scales can be separated. Recall that in the LES approach the small length scales and timescales were filtered out. However, even the intermediate-to-large turbulence scales must be filtered out to obtain a set of equations that can be used for routine simulations. Hence, the solution of these equations remains the only viable means for routine simulations of turbulent flows encountered in engineering practice. More than 100 years ago Reynolds proposed that the instantaneous variables could be split into a mean part and a fluctuating part,

$$U_i = \langle U_i \rangle + u_i \tag{4.36}$$

and

$$P = \langle P \rangle + p. \tag{4.37}$$

This method is therefore referred to as Reynolds decomposition. All turbulence models in the following sections of this chapter share the fact that they are mathematically based on the Reynolds-decomposition concept. With Reynolds decomposition, the flow is described statistically by the mean flow velocity and the turbulence quantities. By time averaging over a reasonable time period the turbulence fluctuations are separated from the non-turbulence quantities. Hence, the set of equations obtained with this method is called the Reynolds averaged Navier–Stokes equations, or simply the RANS equations. In many practical cases it is necessary to simulate non-steady flows, where the instantaneous variables are averaged over a time period that is large compared with the turbulence timescales but small compared with the timescale of the mean components. This means that the time derivative of the mean flow in the RANS equations accounts for variations at timescales larger than those of turbulence.

Recall that for incompressible flows the continuity equation reads

$$\frac{\partial U_j}{\partial x_j} = 0 \tag{4.38}$$

and the Navier–Stokes equations read

$$\frac{\partial U_i}{\partial t} + U_j \frac{\partial U_i}{\partial x_j} = -\frac{1}{\rho}\frac{\partial P}{\partial x_i} + \nu \frac{\partial^2 U_i}{\partial x_j \, \partial x_j}. \tag{4.39}$$

The equations for the mean variables of these quantities are derived by substituting the decomposed form into the Navier–Stokes equations and taking the average. Let us now substitute for the instantaneous variables in Eqs. (4.38) and (4.39) the decomposed variables. By substituting we obtain

$$\frac{\partial(\langle U_i \rangle + u_i)}{\partial x_i} = 0 \tag{4.40}$$

and

$$\frac{\partial(\langle U_i \rangle + u_i)}{\partial t} + (\langle U_j \rangle + u_j)\frac{\partial(\langle U_i \rangle + u_i)}{\partial x_j} = -\frac{1}{\rho}\frac{\partial(\langle P \rangle + p)}{\partial x_i} + \nu \frac{\partial^2(\langle U_i \rangle + u_i)}{\partial x_j \partial x_j}. \tag{4.41}$$

After decomposing the dependent variables into mean and fluctuating quantities we then time-average the equations using the operator

$$\langle \phi \rangle = \frac{1}{\tau}\int_t^{t+\tau} \phi(x, \tilde{t}\,)\mathrm{d}\tilde{t}. \tag{4.42}$$

Equation (4.40) then reads

$$\left\langle \frac{\partial(\langle U_i \rangle + u_i)}{\partial x_i} \right\rangle = 0 \tag{4.43}$$

and Eq. (4.41) becomes

$$\left\langle \frac{\partial(\langle U_i\rangle + u_i)}{\partial t} \right\rangle + \left\langle \left(\langle U_j\rangle + u_j\right) \frac{\partial(\langle U_i\rangle + u_i)}{\partial x_j} \right\rangle = -\frac{1}{\rho} \left\langle \frac{\partial(\langle P\rangle + p)}{\partial x_i} \right\rangle + \nu \left\langle \frac{\partial^2(\langle U_i\rangle + u_i)}{\partial x_j\, \partial x_j} \right\rangle. \tag{4.44}$$

Note that all terms linear in fluctuating variables give zero on averaging:

$$\langle u_i\rangle = \langle u_j\rangle = 0. \tag{4.45}$$

This does not apply for the nonlinear term:

$$\begin{aligned} \langle U_i U_j\rangle &= \left\langle (\langle U_i\rangle + u_i)\left(\langle U_j\rangle + u_j\right)\right\rangle = \left\langle \left(\langle U_i\rangle \langle U_j\rangle + u_j\langle U_i\rangle + u_i\langle U_j\rangle + u_i u_j\right)\right\rangle \\ &= \langle U_i\rangle\langle U_j\rangle + \langle u_j\rangle\langle U_i\rangle + \langle u_i\rangle\langle U_j\rangle + \langle u_i u_j\rangle = \langle U_i\rangle\langle U_j\rangle + \langle u_i u_j\rangle. \end{aligned} \tag{4.46}$$

Equations (4.43) and (4.44) reduce to

$$\frac{\partial\langle U_i\rangle}{\partial x_i} = 0 \tag{4.47}$$

and

$$\frac{\partial\langle U_i\rangle}{\partial t} + \langle U_j\rangle \frac{\partial\langle U_i\rangle}{\partial x_j} + \left\langle \frac{\partial u_i u_j}{\partial x_j} \right\rangle = -\frac{1}{\rho}\frac{\partial\langle P\rangle}{\partial x_i} + \nu \frac{\partial^2\langle U_i\rangle}{\partial x_j\, \partial x_j}. \tag{4.48}$$

By re-arranging we obtain the general form of the RANS equation

$$\frac{\partial\langle U_i\rangle}{\partial t} + \langle U_j\rangle \frac{\partial\langle U_i\rangle}{\partial x_j} = -\frac{1}{\rho}\frac{\partial\langle P\rangle}{\partial x_i} + \nu \frac{\partial^2\langle U_i\rangle}{\partial x_j^2} - \frac{\partial\langle u_i u_j\rangle}{\partial x_j}, \tag{4.49}$$

which can be written as

$$\frac{\partial\langle U_i\rangle}{\partial t} + \langle U_j\rangle \frac{\partial\langle U_i\rangle}{\partial x_j} = -\frac{1}{\rho}\frac{\partial}{\partial x_j}\left\{ \langle P\rangle\delta_{ij} + \mu\left(\frac{\partial\langle U_i\rangle}{\partial x_j} + \frac{\partial\langle U_j\rangle}{\partial x_i} \right) - \rho\langle u_i u_j\rangle \right\}. \tag{4.50}$$

This equation was first derived by Reynolds in 1895 and is very similar to the original Navier–Stokes equations (4.39) apart from the additional term $-\rho\langle u_i u_j\rangle$. This term is referred to as the Reynolds stresses and is very important since it introduces a coupling between the mean and fluctuating parts of the velocity field. Note that sometimes $\langle u_i u_j\rangle$ is referred to as the Reynold stresses even though the precise definition of the Reynolds stresses is $-\rho\langle u_i u_j\rangle$. Since the Reynolds stress term contains products of the velocity fluctuations this term must be modelled in order to close Eq. (4.49). This is the sole purpose of RANS turbulence modelling.

Note that by averaging over all timescales of turbulence one performs averaging over the longest timescales of turbulence. This means that the only dynamic behaviour that will be resolved in the simulations is that of the mean flow. For flows that are statistically steady the Reynolds averaged equations of motion do not resolve any of the dynamics

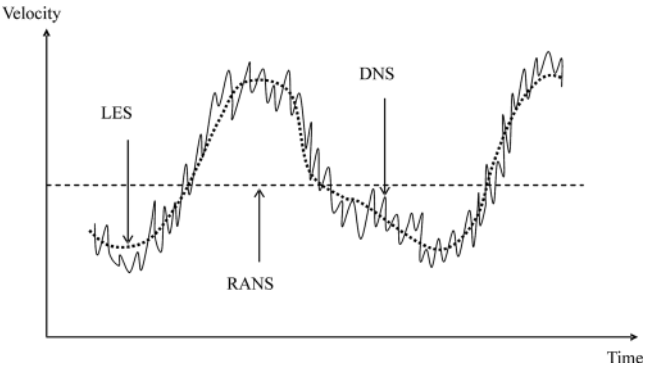

Figure 4.12 One-point representation of resolved turbulence scales in a steady turbulent flow.

even though the effects of turbulence on mass-, momentum- and heat-transfer rates are accounted for. Figure 4.12 illustrates that DNS, LES and RANS resolve scales of different sizes. Note that, while DNS resolves all scales, LES resolves only the largest scales. The non-resolved scales in LES which are more universal can be seen as small-scale fluctuations superposed on the large scales.

Reynolds stresses

Recall that the statistical-averaging process introduced unknown correlations into the mean-flow equations, namely the Reynolds stresses, $\tau_{ij} = -\rho\langle u_i u_j\rangle$. The Reynolds stress term is a second-order tensor that represents a second-order moment of the velocity components at a single point in space. These stresses appear as an additional fictitious stress tensor in Eq. (4.49) by which the fluctuating parts interact and force the mean flow. Therefore they are often called apparent stresses. It is important to point out that, although the Reynolds stress term formally appears similar to the viscous stress term, it is not part of the fluid stress but instead represents the average momentum flux due to the velocity fluctuations, thus characterizing the transfer of momentum by turbulence.

The individual Reynolds stresses in the stress tensor, $\tau_{ij} = -\rho\langle u_i u_j\rangle$, are

$$\tau_{ij} = \begin{bmatrix} -\rho\langle u_1u_1\rangle & -\rho\langle u_1u_2\rangle & -\rho\langle u_1u_3\rangle \\ -\rho\langle u_2u_1\rangle & -\rho\langle u_2u_2\rangle & -\rho\langle u_2u_3\rangle \\ -\rho\langle u_3u_1\rangle & -\rho\langle u_3u_2\rangle & -\rho\langle u_3u_3\rangle \end{bmatrix}. \tag{4.51}$$

Since the Reynolds stress tensor is symmetric, $\langle u_1u_2\rangle = \langle u_2u_1\rangle$, $\langle u_1u_3\rangle = \langle u_3u_1\rangle$ and $\langle u_2u_3\rangle = \langle u_3u_2\rangle$ there are three normal stresses $-\rho\langle u_1u_1\rangle$, $-\rho\langle u_2u_2\rangle$ and $-\rho\langle u_3u_3\rangle$ and three shear stresses $-\rho\langle u_1u_2\rangle$, $-\rho\langle u_1u_3\rangle$ and $-\rho\langle u_2u_3\rangle$. This means that the Reynolds stress tensor contains six unknown terms that must be modelled. One straightforward approach to close Eq. (4.49) would be to derive transport equations for the Reynolds stresses. Unfortunately, this results in third-order moments of the velocity components. An attempt to derive equations describing the evolution of the third-order moments yields equations containing fourth-order moments. This goes on indefinitely and is referred to as the closure problem.

In high-Reynolds-number flows, the Reynolds stress tensor can easily be 1000 times larger than the mean viscous stress tensor,

$$\rho\left\|\left\langle u_i u_j\right\rangle\right\| \gg \mu\left\|\frac{\partial\langle U_i\rangle}{\partial x_j}+\frac{\partial\left\langle U_j\right\rangle}{\partial x_i}\right\|. \tag{4.52}$$

This means that at high Reynolds numbers the viscous stress may generally be neglected when compared with the Reynolds stress insofar as the mean flow equations are concerned. However, this does not apply towards boundaries of the flow. In these regions (thin layers adjacent to the walls) the turbulence is damped, the mean velocity gradients grow larger and the viscous stress becomes comparable to the Reynolds stress. Thus, in this region we have

$$\rho\left\|\left\langle u_i u_j\right\rangle\right\| \approx \mu\left\|\frac{\partial\langle U_i\rangle}{\partial x_j}+\frac{\partial\left\langle U_j\right\rangle}{\partial x_i}\right\|. \tag{4.53}$$

A discussion about these viscous regions and how they can be modelled is given in Section 4.3.

The Boussinesq approximation

To summarize, when the RANS equations were derived we introduced the Reynolds stresses, which are unknown terms, without adding any extra equations. This means that the Reynolds stresses must be modelled since the total number of unknowns is more than the total number of equations. Unless some assumptions are made about the Reynolds stresses it is not possible to solve Eqs. (4.47) and (4.49). One way to model the Reynolds stresses is to relate them to the dependent variables they are meant to transport. Such turbulence models make the prediction of turbulence feasible with a reasonable amount of computer time.

A simple approximation is to express the Reynolds stress tensor, $-\rho\langle u_i u_j\rangle$, in terms of the mean velocity itself. This closure has an approximate character, which means that the solution of the RANS equations is always an approximation. In what follows we consider closures that are based on the concept of turbulent eddy viscosity.

The Boussinesq approximation is based on the assumption that the components of the Reynolds stress tensor are proportional to the mean velocity gradients. The Boussinesq relation proposes that the transport of momentum by turbulence is a diffusive process and that the Reynolds stresses can be modelled using a turbulent viscosity (eddy viscosity), which is analogous to molecular viscosity. The Boussinesq approximation reads

$$\frac{\tau_{ij}}{\rho}=-\left\langle u_i u_j\right\rangle=\nu_{\mathrm{T}}\left(\frac{\partial\langle U_i\rangle}{\partial x_j}+\frac{\partial\left\langle U_j\right\rangle}{\partial x_i}\right)-\frac{2}{3}k\delta_{ij}, \tag{4.54}$$

or

$$\frac{\tau_{ij}}{\rho}=-\left\langle u_i u_j\right\rangle=\nu_{\mathrm{T}}S_{ij}-\frac{2}{3}k\delta_{ij}, \tag{4.55}$$

where

$$S_{ij} = \frac{1}{2}\left(\frac{\partial\langle U_i\rangle}{\partial x_j} + \frac{\partial\langle U_j\rangle}{\partial x_i}\right)$$

is the strain-rate tensor and k is the turbulent kinetic energy per unit mass. The turbulent kinetic energy per unit mass is defined as half the trace of the Reynolds stress tensor $k = \frac{1}{2}\langle u_i u_i\rangle$. In contrast to the molecular viscosity, the turbulent viscosity is not a fluid property but depends strongly on the state of turbulence.

The second term on the right-hand side of Eq. (4.54) represents normal stresses. Thus, a term analogous to the pressure occurs in the usual stress tensor for a viscous fluid, which can be absorbed into the real pressure term. Hence we finally obtain

$$\frac{\partial\langle U_i\rangle}{\partial t} + \langle U_j\rangle\frac{\partial\langle U_i\rangle}{\partial x_j} = -\frac{1}{\rho}\frac{\partial\left(\langle P\rangle + \frac{2}{3}\rho k\right)}{\partial x_i} + \frac{\partial}{\partial x_j}\left[(\nu + \nu_T)\frac{\partial\langle U_i\rangle}{\partial x_j}\right], \quad (4.56)$$

or

$$\frac{\partial\langle U_i\rangle}{\partial t} + \langle U_j\rangle\frac{\partial\langle U_i\rangle}{\partial x_j} = -\frac{1}{\rho}\frac{\partial\langle P\rangle}{\partial x_i} - \frac{2}{3}\frac{\partial k}{\partial x_i} + \frac{\partial}{\partial x_j}\left[(\nu + \nu_T)\left(\frac{\partial\langle U_i\rangle}{\partial x_j} + \frac{\partial\langle U_j\rangle}{\partial x_i}\right)\right]. \quad (4.57)$$

Thus, if specific details of the turbulence are not important we can interpret the fluid itself as a pseudo-fluid with an increased viscosity (effective viscosity, $\nu_{\text{eff}} = \nu + \nu_T$) that roughly approximates the turbulent mixing processes to diffusion of momentum and other flow properties. This means that diffusion models convection, where $\partial\langle u_i u_j\rangle/\partial x_j$ is transport of $\langle U_i\rangle$ in Eq. (4.49).

Regardless of the approach used to determine ν_T, there are several limitations with the Boussinesq approximation. Among others, the Boussinesq approximation assumes that eddies behave like molecules, that turbulence is isotropic and that there exists local equilibrium between stress and strain. As a consequence of these assumptions, predictions of simple flows may fail, e.g. in channel flows, where measurements show that $-\langle u_1^2\rangle \neq -\langle u_2^2\rangle \neq -\langle u_3^2\rangle$. Hence, models that are based on the Boussinesq approximation are limited to prediction of isotropic flows in local equilibrium. Despite the shortcomings of the Boussinesq approximation it is one of the cornerstones in several turbulence models. The reasons for this are the cost of using more elaborate turbulence models and problems with obtaining closures for higher moments.

4.2.4 Models based on the turbulent viscosity hypothesis

Most models evaluating the Reynolds stress tensor simplify the situation through the Boussinesq eddy-viscosity concept. Thus, as part of quantitative turbulence modelling this eddy viscosity, ν_T, must be determined. So when it comes to turbulence modelling based on the RANS equations and the eddy-viscosity concept, the turbulence model can be seen as the set of equations that are needed to determine this viscosity.

As in the kinetic theory of gases, the viscosity is proportional to velocity times distance. The turbulent-viscosity models are based on appropriate velocity, u, and length scales, l, describing the local turbulent viscosity, ν_T. The dimension of ν_T is [m^2 s^{-1}], which means that the product of these two scales gives the right dimension; that is, we have

$$\nu_T = C_\nu \frac{l^2}{t} = C_\nu u l. \tag{4.58}$$

In this expression u and l are the characteristic scales for the large turbulent eddies and C_ν is a proportionality constant. This is reasonable because these scales are responsible for most of the turbulent transport. The turbulent eddy viscosity, ν_T, in Eq. (4.57) may vary with position and time and must be specified before the set of equations can be closed. A proper turbulence model therefore involves a closed set of equations, i.e. the total number of unknown variables equals the total number of equations. There exist numerous methods that provide values for the turbulent viscosity. These methods are usually categorized by the number of additional transport equations that are required for closure, i.e. the equations required to determine the velocity and length scales describing the local turbulence. In the simplest categories of models no additional transport equations are used. These models are therefore referred to as zero-equation models. Furthermore, there are one- and two-equation models in which respectively one and two PDEs are solved together with the RANS equations. The degree of accuracy of each turbulence model depends on the validity of the assumptions behind it. In what follows we will discuss some of the zero-, one- and two-equation models that are used for this purpose. Among these models, the two-equation models are the most widely used for routine simulation of engineering applications.

Zero-, one- and two-equation models

The number of additional PDEs considered in addition to the RANS and continuity equations is used to classify the turbulence models. Hence algebraic models are classified as zero-equation models. One of the most well-known zero-equation models is Prandtl's mixing-length model. In this model ν_T is calculated using an analogy between the chaotic motions of eddies and the random motion of molecules in gases (kinetic gas theory). The mixing length, l, depends strongly on the nature of the flow and is generally space-dependent. This model offers an improvement over the constant-viscosity models and is capable of predicting some simple flows. The motivation for developing more advanced models than the zero-equation models is that it is very difficult to estimate the distribution of the mixing length. Another limitation with this model is that the eddy viscosity is instantaneously affected by the shear rate and vanishes whenever the velocity gradient is zero. This does not agree with experimental data. The reason for this is that the turbulent stresses result not only from events at a single point but also from events in the region, since they are transported by convection and diffusion and they have a certain lifetime before the energy is dissipated. Hence, zero-equation models are unsuitable for general use since they do not account for effects of accumulation and transport on turbulence.

Since turbulent eddies have a certain lifetime and are transported by convection, turbulence is not completely determined by the local conditions but depends also on the history of the eddies. One way to overcome the limitations of the zero-equation models is to relate the turbulent viscosity to a transported turbulent quantity instead of relating it to the mean velocity gradient. In contrast to the zero-equation models the one-equation models allow history effects to be accounted for. It was independently suggested by Kolmogorov and Prandtl that the square root of the time-averaged turbulent kinetic energy, k, should be employed as the characteristic turbulent velocity scale, u. Examples of such models include Prandtl's k–l model and the Spalart–Allmaras model. From the above discussion it can be concluded that transport of the turbulent kinetic energy is taken into account in one-equation models at the cost of solving one additional PDE. The problem with one-equation models is that only the characteristic velocity scale is determined from a transport equation, and the length scale must therefore be specified algebraically. An obvious solution would then be to determine the length scale from an additional transport equation. That is actually what is done in two-equation models.

Two-equation models

Zero- and one-equation models are still used for certain applications but they are rarely used for general-purpose flow simulations. For general-purpose flow simulations, the more sophisticated two-equation models are frequently used. As the number of equations increases, the computational cost increases as well. It should be mentioned that the two-equation models are sometimes referred to as complete models, since they allow the turbulent velocity and length scales to be determined independently. For practical engineering purposes, the most successful models involve two or more transport equations. This is due to the fact that it takes two quantities to characterize the length and velocity scales of turbulent flows. Using transport equations to describe these variables means that the turbulence-production and -dissipation processes can have localized rates. Without the transport mechanism turbulence has to instantly adjust to local conditions, thereby giving unrealistically large production and dissipation rates. In many cases a high local value of turbulence is due to convection of upstream-generated eddies.

A straightforward approach to model the turbulent velocity and length scales is to solve the k equation for the velocity scale and the l equation for the length scale. Usually the names of the turbulence models are logical in the sense that they reflect what is modelled. Hence, a two-equation model that models k and l is simply called a k–l model. More often the second transport equation describes transport of some property other than the length scale, l. Obviously it must be possible to determine the length scale explicitly from this property. Generally we can write an arbitrary property, ϕ, which is related to the length scale, l, in the following way:

$$\phi = k^{\alpha} l^{\beta}. \tag{4.59}$$

Table 4.2 Commonly used properties for determination of the turbulence length scale

α	β	ϕ	Alternative symbol to ϕ	Interpretation of ϕ
0	1	l	l	Length scale
1	−2	k/l^2	ω	Vorticity scale
1/2	−1	$k^{1/2}/l$	f	Frequency scale
−1/2	1	$k^{-1/2}l$	τ	Timescale
3/2	−1	$k^{3/2}/l$	ε	Dissipation rate

This means that for the k–l model $\alpha = 0$ and $\beta = 1$, hence $\phi = l$. There are many possible choices for the second turbulence variable, resulting in different values of α and β. Some of the proposed variables are given in Table 4.2.

The energy-dissipation rate, ε, is the most commonly used of these variables. As implied by its name, the k–ε model describes turbulence using two variables, namely the turbulent kinetic energy, k, and the energy-dissipation rate, ε. The relation between the turbulence length scale and the energy-dissipation rate is

$$\phi = k^{3/2}/l = \varepsilon. \tag{4.60}$$

The length scale is simply the turbulent velocity, $\sqrt{k}$, times the lifetime of the turbulent eddies k/ε,

$$l = \sqrt{k}\frac{k}{\varepsilon} = \frac{k^{3/2}}{\varepsilon}, \tag{4.61}$$

and the turbulent viscosity is given by

$$\nu_\mathrm{T} = C_\nu u l = C_\nu k^{1/2}\frac{k^{3/2}}{\varepsilon} = C_\nu \frac{k^2}{\varepsilon}. \tag{4.62}$$

Two-equation models are widely used for simulation of engineering applications. Even though these models impose limitations, they continue to be favourable since they are robust and inexpensive to implement.

The standard k–ε model

The k–ε model has become very popular due to the important role played by ε in the interpretation of turbulence in addition to the fact that ε appears directly in the transport equation for k. This turbulence model provides a good compromise between generality and economy for many CFD problems. Before looking at the modelled transport equations for k and ε, one should be aware that these equations are actually simplifications of the exact transport equations for k and ε. This means that the k–ε model is one of several possible closures by which the RANS equations are simplified even further. In the following section we will look particularly at the closures introduced to solve the exact k and ε equations. Note that these types of closures are not unique to the k–ε model but are in fact required to close all models that are based on statistical averaging, due the higher-order moments that are introduced. The exact transport equation for the

turbulent kinetic energy, k, can be deduced from the equation for the kinetic energy Eq. (2.26) by Reynolds decomposition and reads

$$\underbrace{\frac{\partial k}{\partial t}}_{\text{I}} + \underbrace{\langle U_j \rangle \frac{\partial k}{\partial x_j}}_{\text{II}} = \underbrace{-\langle u_i u_j \rangle \frac{\partial \langle U_i \rangle}{\partial x_j}}_{\text{III}} \underbrace{- \nu \left\langle \frac{\partial u_i}{\partial x_j} \frac{\partial u_i}{\partial x_j} \right\rangle}_{\text{IV}} + \frac{\partial}{\partial x_j} \left(\underbrace{\nu \frac{\partial k}{\partial x_j}}_{\text{V}} \underbrace{- \frac{\langle u_i u_i u_j \rangle}{2}}_{\text{VI}} \underbrace{- \frac{\langle u_j p \rangle}{\rho}}_{\text{VII}} \right). \tag{4.63}$$

The physical interpretation of the terms in the Eq. (4.63) is as follows.

I. Accumulation of k.
II. Convection of k by the mean velocity.
III. Production of k, large eddies extract energy from the mean flow.
IV. Dissipation of k by viscous stress, whereby turbulent kinetic energy is transformed into heat.
V. Molecular diffusion of k.
VI. Turbulent transport by velocity fluctuations.
VII. Turbulent transport by pressure fluctuations.

In Eq. (4.63) the terms III, IV, VI and VII are unknown and, unless some approximations are introduced, it is not possible to solve this equation. Hence, closures are required for the production, dissipation and diffusion terms. The production term represents the production of turbulent kinetic energy due to the mean flow strain rate. If the equation for the kinetic energy of the mean flow is considered, this term actually appears as a sink in the equation. This clearly shows that the production of turbulent kinetic energy is indeed a result of the mean flow losing kinetic energy, recalling that $\langle E \rangle = \overline{E} + k$. Note that the production term is the Reynolds stresses times the shear rates and maximum production will occur where both are large. This is mainly in the boundary layers close to the walls, and for flow parallel to the wall the maximum production is at $y^+ \approx 12$. The Reynolds stresses can be identified in the production term and it is assumed that the Boussinesq approximation can be used to model this term by relating it to gradients of the mean flow

$$-\langle u_i u_j \rangle = \nu_\mathrm{T} \left(\frac{\partial \langle U_i \rangle}{\partial x_j} + \frac{\partial \langle U_j \rangle}{\partial x_i} \right) - \frac{2}{3} k \delta_{ij}. \tag{4.64}$$

This means that the production of turbulent kinetic energy can be modelled as

$$-\langle u_i u_j \rangle \frac{\partial \langle U_i \rangle}{\partial x_j} = \nu_\mathrm{T} \left(\frac{\partial \langle U_i \rangle}{\partial x_j} + \frac{\partial \langle U_j \rangle}{\partial x_i} \right) \frac{\partial \langle U_i \rangle}{\partial x_j} - \frac{2}{3} k \frac{\partial \langle U_i \rangle}{\partial x_i}. \tag{4.65}$$

Note that the last term in Eq. (4.65) is zero for incompressible flow due to continuity. It is important to recall that the Boussinesq approximation is an isotropic model for the Reynolds stresses and assumes that the normal stresses are all equal.

The second closure needed to model the k equation is a relation for the energy-dissipation rate, which is the rate of destruction of turbulent kinetic energy. Note that the energy dissipation of turbulent kinetic energy is defined as

$$\varepsilon = \nu \left\langle \frac{\partial u_i}{\partial x_j} \frac{\partial u_i}{\partial x_j} \right\rangle. \tag{4.66}$$

The third closure is required to describe the turbulent transport of k. These higher-order moments (terms VI and VII) are usually modelled by assuming a gradient-diffusion transport mechanism. This assumption allows the turbulent transport due to velocity and pressure fluctuations to be modelled as

$$-\frac{\langle u_i u_i u_j \rangle}{2} - \frac{\langle u_j p \rangle}{\rho} = \frac{\nu_\mathrm{T}}{\sigma_k} \frac{\partial k}{\partial x_j}. \tag{4.67}$$

Here, σ_k is a model coefficient known as the Prandtl–Schmidt number and ν_T is the turbulent viscosity. Substituting these closures into the exact transport equation for k gives the modelled equation for k

$$\frac{\partial k}{\partial t} + \langle U_j \rangle \frac{\partial k}{\partial x_j} = \nu_\mathrm{T} \left[\left(\frac{\partial \langle U_i \rangle}{\partial x_j} + \frac{\partial \langle U_j \rangle}{\partial x_i} \right) \frac{\partial \langle U_i \rangle}{\partial x_j} \right] - \varepsilon + \frac{\partial}{\partial x_j} \left[\left(\nu + \frac{\nu_\mathrm{T}}{\sigma_k} \right) \frac{\partial k}{\partial x_j} \right]. \tag{4.68}$$

To close the k equation we need to calculate ε and the turbulent viscosity. Obviously, the energy-dissipation rate is modelled with a second transport equation. Note that the production of turbulent kinetic energy is modelled as the product of the turbulent viscosity and average velocity gradients.

The exact ε equation can be written as

$$\begin{aligned}
&\underbrace{\frac{\partial \varepsilon}{\partial t}}_{\mathrm{I}} + \underbrace{\langle U_j \rangle \frac{\partial \varepsilon}{\partial x_j}}_{\mathrm{II}} \\
&= \underbrace{-2\nu \left(\left\langle \frac{\partial u_i}{\partial x_k} \frac{\partial u_j}{\partial x_k} \right\rangle + \left\langle \frac{\partial u_k}{\partial x_i} \frac{\partial u_k}{\partial x_j} \right\rangle \right) \frac{\partial \langle U_i \rangle}{\partial x_j}}_{\mathrm{III}} \underbrace{- 2\nu \left\langle u_k \frac{\partial u_i}{\partial x_j} \right\rangle \frac{\partial^2 \langle U_i \rangle}{\partial x_k \partial x_j}}_{\mathrm{IV}} \\
&\quad \underbrace{- 2\nu \left\langle \frac{\partial u_i}{\partial x_k} \frac{\partial u_i}{\partial x_j} \frac{\partial u_k}{\partial x_j} \right\rangle}_{\mathrm{V}} \underbrace{- 2\nu\nu \left\langle \frac{\partial^2 u_i}{\partial x_k \partial x_j} \frac{\partial^2 u_i}{\partial x_k \partial x_j} \right\rangle}_{\mathrm{VI}} \\
&\quad + \frac{\partial}{\partial x_j} \left(\underbrace{\nu \frac{\partial \varepsilon}{\partial x_j}}_{\mathrm{VII}} \underbrace{- \nu \left\langle u_j \frac{\partial u_i}{\partial x_j} \frac{\partial u_i}{\partial x_j} \right\rangle}_{\mathrm{VIII}} \underbrace{- 2\frac{\nu}{\rho} \left\langle \frac{\partial p}{\partial x_j} \frac{\partial u_j}{\partial x_j} \right\rangle}_{\mathrm{IX}} \right).
\end{aligned} \tag{4.69}$$

The physical interpretation of some of the terms in Eq. (4.69) is as follows.

I. Accumulation of ε.
II. Convection of ε by the mean velocity.
III and IV. Production of dissipation, due to interactions between the mean flow and the products of the turbulent fluctuations.
V and VI. Destruction rate of the dissipation, due to turbulent velocity fluctuations.
VII. Viscous diffusion of ε.
VIII. Turbulent transport of ε due to velocity fluctuations.
IX. Turbulent transport of ε due to pressure–velocity fluctuations.

In Eq. (4.69) there are several unknown terms containing correlations of fluctuating velocities and gradients of fluctuating velocities and pressure, namely terms III, IV, V, VI, VIII and IX. Again we need several closures for the unknown terms in order to close the equation. The result of introducing closures is that the modelled equation is drastically simplified. To avoid tedious manipulation of the exact ε equation we simply give the general form of the modelled ε equation:

$$\underbrace{\frac{\partial \varepsilon}{\partial t}}_{\mathrm{I}} + \underbrace{\langle U_j \rangle \frac{\partial \varepsilon}{\partial x_j}}_{\mathrm{II}} = \underbrace{C_{\varepsilon 1} \nu_{\mathrm{T}} \frac{\varepsilon}{k} \left[\left(\frac{\partial \langle U_i \rangle}{\partial x_j} + \frac{\partial \langle U_j \rangle}{\partial x_i} \right) \frac{\partial \langle U_i \rangle}{\partial x_j} \right]}_{\mathrm{III}} - \underbrace{C_{\varepsilon 2} \frac{\varepsilon^2}{k}}_{\mathrm{IV}} + \underbrace{\frac{\partial}{\partial x_j} \left[\left(\nu + \frac{\nu_{\mathrm{T}}}{\sigma_\varepsilon} \right) \frac{\partial \varepsilon}{\partial x_j} \right]}_{\mathrm{V}}. \tag{4.70}$$

The physical interpretation of the terms in Eq. (4.70) is as follows.

I. Accumulation of ε.
II. Convection of ε by the mean velocity.
III. Production of ε.
IV. Dissipation of ε.
V. Diffusion of ε.

The time constant for turbulence is calculated from the turbulent kinetic energy and the rate of dissipation of turbulent kinetic energy:

$$\tau = k/\varepsilon. \tag{4.71}$$

Note that the source term in the ε equation is the same as that in the k equation divided by the time constant τ in Eq. (4.71) and the rate of dissipation of ε is proportional to

$$\varepsilon/\tau = \varepsilon^2/k. \tag{4.72}$$

The turbulent viscosity must be calculated to close the k–ε model. Recall that the turbulent viscosity is given as the product of the characteristic velocity and length scales, $\nu_{\mathrm{T}} \propto ul$. This means that we have

$$\nu_{\mathrm{T}} = C_\mu \frac{k^2}{\varepsilon}. \tag{4.73}$$

Table 4.3 Closure coefficients in the standard k–ε model

Constant	Value
C_μ	0.09
$C_{\varepsilon 1}$	1.44
$C_{\varepsilon 2}$	1.92
σ_k	1.00
σ_ε	1.30

Finally, the five closure coefficients (C_μ, $C_{\varepsilon 1}$, $C_{\varepsilon 2}$, σ_k and σ_ε) in the k–ε model are assumed to be universal and thus constant, although they can vary slightly from one flow to another. The values for these constants are given in Table 4.3.

The robustness and the easily interpreted model terms make the k–ε model the most widely used two-equation model. However, the standard k–ε model does not always give good accuracy. Examples of flows that cannot be predicted accurately with the standard k–ε model are flows with streamline curvature, swirling flows and axisymmetric jets. The inaccuracies stem from the underlying Boussinesq hypothesis which imposes isotropy and from the way in which the dissipation equation is modelled. Actually this model was derived and tuned for flows with high Reynolds numbers. This implies that it is suited for flows in which the turbulence is nearly isotropic and flows in which the energy cascade proceeds in local equilibrium with respect to generation. Furthermore, the model parameters in the k–ε model are a compromise to give the best performance for a wide range of different flows. The accuracy of the model can therefore be improved by adjusting the parameters for particular experiments. As the strength and weaknesses of the standard k–ε model have become known, improvements have been made to the model to improve its performance. In the literature, numerous modifications for the turbulence models have been suggested. The most well-known variants of the standard model are the RNG and the realizable k–ε models. It is not within the scope of this book to discuss all these modifications; however, a closer look will be taken at the RNG and realizable k–ε models. In fact, the k–ε model and its variants have become a workhorse in practical engineering flow simulations.

The RNG k–ε model

The main physical difference between the standard model and the RNG k–ε model lies in a different formulation of the dissipation equation. In the RNG k–ε model, an additional source term, S_ε, is added and the equation is given by

$$\frac{\partial \varepsilon}{\partial t} + \langle U_j \rangle \frac{\partial \varepsilon}{\partial x_j} = C_{\varepsilon 1} \nu_\mathrm{T} \frac{\varepsilon}{k} \left[\left(\frac{\partial \langle U_i \rangle}{\partial x_j} + \frac{\partial \langle U_j \rangle}{\partial x_i} \right) \frac{\partial \langle U_i \rangle}{\partial x_j} \right] - C_{\varepsilon 2} \frac{\varepsilon^2}{k} + \frac{\partial}{\partial x_j} \left[\left(\nu + \frac{\nu_\mathrm{T}}{\sigma_\varepsilon} \right) \frac{\partial \varepsilon}{\partial x_j} \right] - S_\varepsilon, \tag{4.74}$$

where the source term S_ε is given by

$$S_\varepsilon = 2\nu S_{ij} \left\langle \frac{\partial u_l}{\partial x_i} \frac{\partial u_l}{\partial x_j} \right\rangle . \tag{4.75}$$

In the RNG k–ε model the additional term, S_ε, is modelled as

$$S_\varepsilon = \frac{C_\mu \eta^3 (1 - \eta/\eta_0)\, \varepsilon^2}{\left(1 + \beta\eta^3\right) k}. \tag{4.76}$$

Here

$$\eta = \frac{k}{\varepsilon} \sqrt{2 S_{ij} S_{ij}}$$

and S_{ij} is the strain-rate tensor. The constants η_0 and β take the values 4.38 and 0.012, respectively. This additional term is an ad-hoc model that is largely responsible for the differences in performance compared with the standard model.

The standard k–ε model is known to be too dissipative, namely the turbulent viscosity in recirculations tends to be too high, thus damping out vortices. In regions with large strain rate the additional term in the RNG model results in smaller destruction of ε, hence augmenting ε and reducing k, which in effect reduces the effective viscosity. Improvements can therefore be expected for swirling flows and flows in which the geometry has a strong curvature. Hence the RNG model is more responsive to the effects of rapid strain and streamline curvature than the standard k–ε model. Although the RNG model is very good for predicting swirling flows, its predictions for jets and plumes are inferior to the standard k–ε model. By using a mathematical renormalization-group (RNG) technique, the k–ε model can be derived from the Navier–Stokes equation, which results in different, analytical, model constants. The constants stemming from the RNG analysis differ slightly from the empirically determined constants in the standard k–ε model.

The realizable k–ε model

The realizable model differs from the standard k–ε model in that it features a realizability constraint on the predicted stress tensor, thereby giving it the name of realizable k–ε model. The difference comes from a correction of the k equation where the normal stress can become negative in the standard k–ε model for flows with large mean strain rates. This can be seen by analysing the normal components of the Reynolds stress tensor:

$$\langle u_i u_i \rangle = \sum_i \langle u_i^2 \rangle = \frac{2}{3} k - 2\nu_\mathrm{T} \frac{\partial \langle U_i \rangle}{\partial x_j}. \tag{4.77}$$

Note that the normal stress $\langle u_i u_i \rangle$ must be larger than zero by definition, since it is a sum of squares. However, Eq. (4.77) implies that, if the strain is sufficiently large, the normal stress becomes negative. The realizable k–ε model uses a variable C_μ so that this

will never occur. In fact, C_μ is no longer taken to be a constant; instead, it is a function of the local state of the flow to ensure that the normal stresses are positive under all flow conditions, i.e. to ensure realizability. In other words, the realizable k–ε model ensures that the normal stresses are positive, i.e. $\langle u_i^2 \rangle \geq 0$. Neither the standard nor the RNG k–ε model is realizable. Realizability also means that the stress tensor satisfies $\langle u_i^2 \rangle \langle u_j^2 \rangle - \langle u_i u_j \rangle^2 \geq 0$, i.e. Schwarz's inequality is fulfilled. Hence, the model is likely to provide better performance for flows involving rotation and separation.

In addition, this model generally involves a modification of the ε equation. This modification involves a production term for turbulent energy dissipation that is not found in either the standard or the RNG model. The standard k–ε model predicts the spreading rate in planar jets reasonably well, but poorly predicts the spreading rate for axisymmetric jets. This is considered to be mainly due to the modelled dissipation equation. It is noteworthy that the realizable k–ε model resolves the round-jet anomaly, i.e. it predicts the spreading rate for axisymmetric jets as well as for planar jets. It is important to realize that this model is better suited to flows in which the strain rate is large. This includes flows with strong streamline curvature and rotation. Validation of complex flows, e.g. boundary-layer flows, separated flows and rotating shear flows, has shown that the realizable k–ε model performs better than the standard k–ε model.

The k–ω models

Another popular two-equation model is the k–ω model. In this turbulence model the specific dissipation, ω, is used as the length-determining quantity. This quantity is called specific dissipation by definition, where $\omega \propto \varepsilon / k$, and it should be interpreted as the inverse of the timescale on which dissipation occurs. The modelled k equation is

$$\frac{\partial k}{\partial t} + \langle U_j \rangle \frac{\partial k}{\partial x_j} = \nu_\mathrm{T} \left[\left(\frac{\partial \langle U_i \rangle}{\partial x_j} + \frac{\partial \langle U_j \rangle}{\partial x_i} \right) \frac{\partial \langle U_i \rangle}{\partial x_j} \right] - \beta k \omega + \frac{\partial}{\partial x_j} \left[\left(\nu + \frac{\nu_\mathrm{T}}{\sigma_k} \right) \frac{\partial k}{\partial x_j} \right] \tag{4.78}$$

and the modelled ω equation is

$$\frac{\partial \omega}{\partial t} + \langle U_j \rangle \frac{\partial \omega}{\partial x_j} = \alpha \frac{\omega}{k} \nu_\mathrm{T} \left[\left(\frac{\partial \langle U_i \rangle}{\partial x_j} + \frac{\partial \langle U_j \rangle}{\partial x_i} \right) \frac{\partial \langle U_i \rangle}{\partial x_j} \right] - \beta^* \omega^2 + \frac{\partial}{\partial x_j} \left[\left(\nu + \frac{\nu_\mathrm{T}}{\sigma_\omega} \right) \frac{\partial \omega}{\partial x_j} \right], \tag{4.79}$$

where the turbulent viscosity is calculated from

$$\nu_\mathrm{T} = \frac{k}{\omega}. \tag{4.80}$$

An advantage of this model compared with the k–ε model is the performance in regions with low turbulence when both k and ε approach zero. This causes problems because both k and ε must go to zero at a correct rate since the dissipation term in the ε equation

includes ε^2/k. In contrast, no such problems occur in the k–ω model. Furthermore, the k–ω model has been shown to reliably predict the law of the wall when the model is used in the viscous sub-layer, thereby eliminating the need to use wall functions, except for computational efficiency. The k–ω model proves to be superior in this area due to the fact that the k–ε model requires either a low-Reynolds-number modification or the use of wall functions when applied to wall-bounded flows. However, the low-*Re* k–ω model requires a very fine mesh close to the wall with the first grid below $y^+ = 5$.

For constant-pressure boundary-layer flow, both the k–ε model and the k–ω model give good predictions. However, for boundary layers with adverse pressure gradients the k–ω model is claimed to give better predictions. For further information the reader is referred to [12].

4.2.5 Reynolds stress models (RSMs)

Turbulence models based on the Boussinesq approximation are inaccurate for flows with sudden changes in the mean strain rate. This is because history effects of the Reynolds stresses persist for long distances in turbulent flows due to a relatively slow exchange of momentum between eddies. Recall that the Boussinesq approximation assumes that eddies behave like molecules and exchange momentum quickly. In the Reynolds stress models, the isotropic eddy-viscosity concept, which is the primary weakness of the two equation models, is not used. Abandoning the isotropic eddy-viscosity concept, the RSM closes the RANS equations via solution of the transport equations for Reynolds stresses, $\tau_{ij} = -\rho\langle u_i u_i\rangle$, and for the energy-dissipation rate, ε. The RSM solves one equation for each Reynolds stress and hence does not need any modelling of the turbulence to the first order. The Reynolds stress models are nonlinear eddy-viscosity models, and are usually referred to as second-moment closures (second-order closures) since the only terms modelled are of third order or higher. The primary advantage of stress-transport models is the natural approach in which non-local and history effects are accounted for. These models can significantly improve the performance under certain conditions, since they account for effects of streamline curvature, swirl, rotation and rapid changes in strain rate in a more rigorous manner than do the two-equation models. In principle, stress-transport modelling is a much better approach but the problem is in providing closures to the extra unknown correlations that arise in the derivation of the exact equations. The interest in using Reynolds stress-transport equations is also held back by the fact that these equations are much more expensive to compute, since $6 + 1$ additional PDEs are solved, and they are susceptible to numerical instability since they are strongly coupled. However, the Reynolds stress model must be used when the flow features of interest are the result of anisotropy in the Reynolds stresses.

Stress-transport modelling

The stress-transport model solves one transport equation for each Reynolds stress. The equations describing the transport of Reynolds stresses can be obtained directly from the Navier–Stokes equations by using the Reynolds decomposition and averaging.

The complete transport equations for the Reynolds stresses are

$$\underbrace{\frac{\partial \langle u_i u_j \rangle}{\partial t}}_{\text{I}} + \underbrace{\langle U_k \rangle \frac{\partial \langle u_i u_j \rangle}{\partial x_k}}_{\text{II}} = \underbrace{-\left(\langle u_i u_k \rangle \frac{\partial \langle U_j \rangle}{\partial x_k} + \langle u_j u_k \rangle \frac{\partial \langle U_i \rangle}{\partial x_k} \right)}_{\text{III}}$$
$$\underbrace{-2\nu \left\langle \frac{\partial u_i}{\partial x_k} \frac{\partial u_j}{\partial x_k} \right\rangle}_{\text{IV}} + \underbrace{\left\langle \frac{p}{\rho} \left(\frac{\partial u_i}{\partial x_j} + \frac{\partial u_j}{\partial x_i} \right) \right\rangle}_{\text{V}}$$
$$\underbrace{-\frac{\partial}{\partial x_k} \left(\langle u_i u_j u_k \rangle + \delta_{ik} \frac{\langle u_j p \rangle}{\rho} + \delta_{jk} \frac{\langle u_i p \rangle}{\rho} - \nu \frac{\partial \langle u_i u_j \rangle}{\partial x_k} \right)}_{\text{VI}}. \tag{4.81}$$

The terms in Eq. (4.81) represent the following effects.

I. Accumulation of $\langle u_i u_j \rangle$.
II. Convection of $\langle u_i u_j \rangle$ by the mean velocity.
III. Production of $\langle u_i u_j \rangle$, generation rate of the turbulent stresses by mean shear, large eddies extract energy from the mean flow strain rate.
IV. Viscous dissipation of $\langle u_i u_j \rangle$, dissipation rate of turbulent stresses, whereby turbulent kinetic energy is transformed into heat.
V. Pressure–strain correlation, which gives redistribution among the Reynolds stresses.
VI. Transport terms, all terms except the last term, which is molecular diffusion, account for turbulent transport.

Equation (4.81) may be written in the following shorthand notation:

$$\frac{\partial \langle u_i u_j \rangle}{\partial t} + \langle U_k \rangle \frac{\partial \langle u_i u_j \rangle}{\partial x_k} = P_{ij} - \varepsilon_{ij} + \phi_{ij} + d_{ij}. \tag{4.82}$$

The physical interpretation of Eq. (4.82) is that the individual stresses are generated, convected and dissipated at different rates. Hence, the modelling is at a higher fundamental level than the approach of obtaining a turbulent viscosity. Consequently, the eddy-viscosity hypothesis is not needed, which eliminates one of the major shortcomings of the models described in the previous section. The main difference between the turbulent kinetic energy and stress equations is term V, which has no equivalent in the k equation. This term is called the pressure–strain or pressure-scrambling term. The term acts to redistribute turbulent energy from one stress component to another. This concept can be shown through a summation of the equations for the normal stresses by using the continuity of the diagonal elements

$$\phi_{ii} = \left\langle \frac{p}{\rho} \left(\frac{\partial u_i}{\partial x_i} + \frac{\partial u_i}{\partial x_i} \right) \right\rangle = 0. \tag{4.83}$$

This means that, if the normal stress in one direction is less than that in the other direction, it will receive energy through ϕ_{ij}. Thus, this process can be thought of as

redistributive, tending to return the turbulence to an isotropic state, with no direct influence on the level of turbulence energy.

Equation (4.81) gives six equations for the Reynolds stresses. Note that terms I, II and III are exact in that they contain only the Reynolds stresses and the mean strains. Except for the first three terms, all other terms must be modelled. Actually, it is possible to derive a set of equations for the unknowns. However, this will merely introduce higher-order terms that require closure. Hence, at some level, turbulence models must be introduced in order to close the set of equations.

The dissipative terms are modelled assuming that they are isotropic since the dissipative processes occur at the smallest scales,

$$\varepsilon_{ij} = 2\nu \left\langle \frac{\partial u_i}{\partial x_k} \frac{\partial u_j}{\partial x_k} \right\rangle = \frac{2}{3}\varepsilon\delta_{ij}. \tag{4.84}$$

Here the energy dissipation, ε, is obtained from its own transport equation.

The contributions from turbulence–turbulence interactions and from mean strains are usually accounted for in modelling of the pressure–strain term as

$$\phi_{ij} = \left\langle \frac{p}{\rho} \left(\frac{\partial u_i}{\partial x_j} + \frac{\partial u_j}{\partial x_i} \right) \right\rangle = \phi_{ij1} + \phi_{ij2}. \tag{4.85}$$

Here, ϕ_{ij1} is the slow pressure–strain term which serves to redistribute energy among the Reynolds stresses and ϕ_{ij2} is the rapid pressure–strain term which counteracts the production of anisotropy. The term giving a return to isotropy, or slow pressure–strain term, ϕ_{ij1}, is modelled as

$$\phi_{ij1} = -c_1\varepsilon \left(\frac{\langle u_i u_j \rangle}{k} - \frac{2}{3}\delta_{ij} \right) \tag{4.86}$$

and the rapid pressure–strain term, ϕ_{ij2}, is modelled as

$$\phi_{ij2} = -c_2 \left(P_{ij} - \frac{2}{3} P_{kk}\delta_{ij} \right), \tag{4.87}$$

where

$$P_{ij} = -\left(\langle u_i u_k \rangle \frac{\partial \langle U_j \rangle}{\partial x_k} + \langle u_j u_k \rangle \frac{\partial \langle U_i \rangle}{\partial x_k} \right). \tag{4.88}$$

The turbulent transport terms are often modelled on the basis of a gradient-diffusion hypothesis

$$\langle u_k \phi \rangle \propto -\frac{k}{\varepsilon} \langle u_k u_l \rangle \frac{\partial \phi}{\partial x_l} \tag{4.89}$$

and assuming a negligible pressure-diffusion. Hence, the term is modelled as

$$\begin{aligned} d_{ij} &= -\frac{\partial}{\partial x_k} \left(\langle u_i u_j u_k \rangle + \delta_{ik} \frac{\langle u_j p \rangle}{\rho} + \delta_{jk} \frac{\langle u_i p \rangle}{\rho} - \nu \frac{\partial \langle u_i u_j \rangle}{\partial x_k} \right) \\ &= \frac{\partial}{\partial x_k} \left(c_s \frac{k}{\varepsilon} \langle u_k u_l \rangle \frac{\partial \langle u_i u_j \rangle}{\partial x_l} \right). \end{aligned} \tag{4.90}$$

Note that it is good practice to include wall correction terms in the modelled equations to account for wall reflection effects. Note also that an additional transport equation for the energy-dissipation rate is solved. Thus, we have a solvable set of equations, e.g. 11 equations for 11 unknowns, $\langle U_i \rangle$, $\langle u_i u_j \rangle$, $\langle P \rangle$ and ε.

4.2.6 Advanced turbulence modelling

Turbulence models that fall beyond the bounds of the categories presented earlier have been developed. It is difficult to sum up all the progress in this field in a few sentences; instead, the interested reader is referred to textbooks on advanced turbulence modelling for further insight into this exciting area. It should also be mentioned that research in this area still remains active.

4.2.7 Comparisons of various turbulence models

In the previous sections, we have presented turbulence models that are commonly encountered in commercial CFD codes. In these sections the physical and mathematical principles underlying the turbulence models were presented together with discussions about their limitations. Table 4.4 gives a short summary of the advantages and shortcomings of these models.

In general the turbulence models are developed to predict velocities accurately. The parameters in the models, e.g. k and ε, may very well be off by a factor of 3. Using these parameters in other models, e.g. for mixing or bubble break-up, should be done with the awareness that the parameters do not have exact physical relevance but only show the trend.

4.3 Near-wall modelling

Most flows of engineering interest involve situations in which the flow is constrained by a solid wall. Ludwig Prandtl was the first to realize that the relative magnitude of the inertial and viscous forces changed on going from a layer near the wall to a region far from the wall. In the early 1900s he presented the theory which describes boundary-layer effects. The wall no-slip condition ensures that, over some region of the wall layer, viscous effects on the transport processes must be large. Recall that particular turbulence models such as the k–ε model are not valid in the near-wall region, where viscous effects are dominant. Furthermore, rapid variation of the flow variables occurs within this region. This implies that a very fine computational mesh is required in order to resolve the steep gradients of the flow variables accurately. Representation of these processes within a CFD model raises problems. Basically, there are two approaches that can be used to model the near-wall region. In the first approach the viscosity-affected near-wall region is not resolved. Instead, wall functions are used to obtain boundary conditions for the mean velocity components and the turbulent quantities at the first

Table 4.4 General advantages and disadvantages for different classes of turbulence models

Turbulence model	Advantages	Shortcomings/limitations
Zero-equation models, e.g. mixing-length model	Cost-effective model applicable for a limited number of flows.	When $\partial U/\partial y = 0 \Rightarrow \nu_T = 0$. Lack of transport of turbulent scales. Estimation of the mixing length is difficult. Cannot be used as a general turbulence model.
One-equation models, e.g. k-algebraic model	Cost-effective model applicable for a limited number of flows.	The use of an algebraic equation for the length scale is too restrictive. Transport of the length scale is not accounted for.
Two-equation models, k–ε group standard, RNG, realizable, k–ω and SST	Complete models in the sense that velocity and length scales of turbulence are predicted with transport equations. Good results for many engineering applications. Especially good for trend analysis. Robust, economical and easy to apply.	Limited to an eddy-viscosity assumption. Turbulent viscosity is assumed to be isotropic. Convection and diffusion of the shear stresses are neglected.
Standard k–ε	The most widely used and validated model.	Not good for round jets and flows involving significant curvature, swirl, sudden acceleration, separation and low-Re regions.
RNG k–ε	Modification of the standard k–ε model gives improved simulations for swirling flows and flow separation.	Not as stable as the standard k–ε model. Not suited for round jets.
Realizable k–ε	Modification of the standard k–ε model gives improved simulations for swirling flows and flow separation. Can also handle round jets.	Not as stable as the standard k–ε model.
k–ω model	Works well at low Re. Does not need wall functions. Works well with adverse pressure gradients and separating flow.	Needs fine mesh close to the wall, first grid point at $y^+ < 5$.
SST model	Uses k–ε in the free stream and k–ω in the wall-bounded region. Works well with adverse pressure gradients and separating flow. Many authors recommend that the SST model should replace the k–ε model as the first choice.	Needs fine mesh close to the wall. Overpredicts turbulence in regions with large normal strain, e.g. stagnation regions and regions with strong acceleration, but is better than k–ε.
Reynolds stress models, (RSMs)	Applicable for complex flow where the turbulent-viscosity models fail. Accounts for anisotropy. Good performance for many complex flows, e.g. swirl, flow separation and planar jets.	Computationally expensive with 11 transport equations. Several terms in the transport equations must be closed. Poor performance for some flows due to the closures introduced in the model.

Table 4.4 (*cont.*)

Turbulence model	Advantages	Shortcomings/limitations
Large-eddy Simulation (LES)	Applicable to complex flows. Gives information about structures in turbulent flows. Gives a lot of information that cannot be obtained otherwise.	High computational cost. Large amount of data that must be stored and post-processed. Difficult to find proper time-resolved boundary conditions for flow.
DNS	No turbulence models are introduced. Useful at low Re numbers, especially for gaseous flows. Useful to develop and validate turbulence models.	Extreme computational cost for practical engineering flow simulations. Huge amount of data.

grid point far from the wall. The other approach involves modification of the turbulence models, which allows the viscosity-affected region to be resolved.

4.3.1 Turbulent boundary layers

At a solid wall, the relative velocity between the fluid and the wall is zero. This is called the 'no-slip condition'. The relative velocity is zero because molecules, moving with random motions plus the mean fluid velocity, hit the solid wall and all the relative momentum is lost, being transferred to the solid wall. Molecules bouncing back into the flow slow down the fluid in the wall layer. Thus, a 'boundary layer' is created. In this region the velocity increases rapidly from zero at the wall to the free-stream velocity. Note that boundary layers may be either laminar or turbulent, depending on the Reynolds number. Turbulent boundary layers, from high Reynolds numbers, are characterized by unsteady swirling flows inside the boundary layer, which give higher mass-, momentum- and heat-transfer rates than apply to a laminar boundary layer, which arises from a low Reynolds number. The efficient momentum transport in turbulent boundary layers increases the wall shear stress. Thus, at high Reynolds numbers we encounter turbulent boundary layers, which produce a greater drag. Hence, details of the flow within boundary layers may be very important in many CFD simulations.

Turbulent boundary layers, of thickness δ, can be divided into an inner region, $0 < y < 0.2\delta$, and an outer region, $0.2\delta < y < \delta$, as shown in Figure 4.13.

It is common practice to divide the inner region into sub-layers on the basis of the relative magnitude of the viscous and turbulent parts of the total shear stress, τ_{xy},

$$\tau_{xy} = \rho\nu\frac{\mathrm{d}\langle U_x\rangle}{\mathrm{d}y} - \rho\langle u_x u_y\rangle. \tag{4.91}$$

In the innermost layer, the viscous sub-layer, the flow is almost laminar and molecular viscosity plays a dominant role in momentum transfer. The viscous sub-layer is defined as the region where the viscous stress is dominant. Near the wall, viscous damping reduces the tangential velocity fluctuations, while kinematic blocking reduces the normal

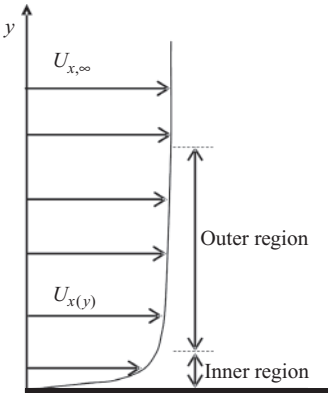

Figure 4.13 The boundary layer in a turbulent flow.

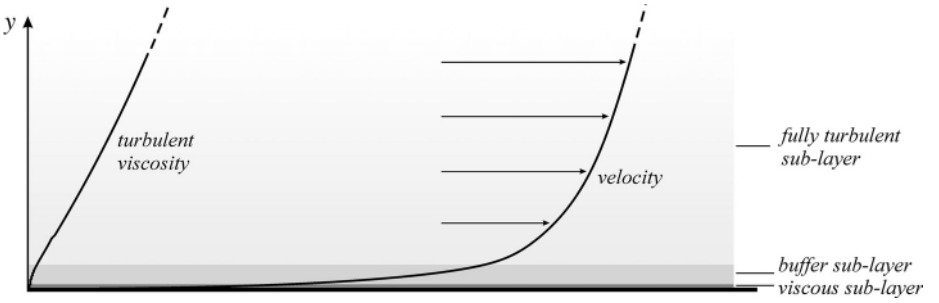

Figure 4.14 Sub-layers in the inner region.

fluctuations. Note that the boundary conditions of the velocities, u_x, $u_y \to 0$ as $y \to 0$, imply that the Reynolds stresses vanish rapidly as the wall is approached. At the wall the stress is entirely due to viscous shear,

$$\tau_w = \rho\nu \left.\frac{\mathrm{d}\langle U_x\rangle}{\mathrm{d}y}\right|_{y=0}. \tag{4.92}$$

In fact, the turbulence in the boundary layer takes its origin from this region. But almost all turbulent eddies are aligned with the wall, and the effective turbulence perpendicular to the wall is almost zero in the vicinity of the wall. Further away from the wall, the viscous and turbulent stresses are equally important. This interim region is the transition layer often referred to as the buffer layer. At even larger distances from the wall the turbulent stresses become dominant. This region is called the fully turbulent layer. Here turbulence plays a major role and viscous effects are negligible. Figure 4.14 shows the three sub-layers.

It is common practice to express the physical extent of these sub-layers in terms of wall variables. The characteristic velocity scale for the sub-layers is given by

$$u_* = \sqrt{\tau_\mathrm{w}/\rho}, \tag{4.93}$$

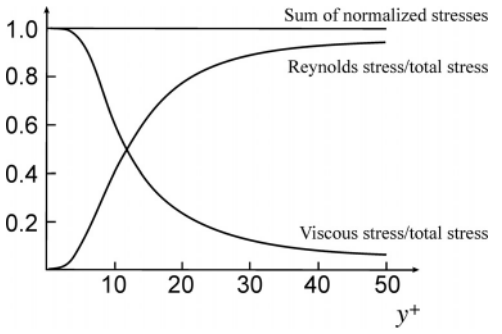

Figure 4.15 Near-wall stresses in the inner region of the turbulent boundary layer.

where u_* is the wall friction velocity, which is of the same order as the r.m.s. value of the velocity fluctuations. This allows us to define a characteristic wall length scale as

$$l_* = \nu/u_*. \tag{4.94}$$

Note that the Reynolds number based on u_* and l_* is equal to one, thus l_* determines the domain of the flow which is significantly affected by the viscosity. On the basis of the characteristic velocity and length scales it is common to use scaled variables to express the physical extent of the sub-layers:

$$u^+ = U/u_* \tag{4.95}$$

and

$$y^+ = y/l_* = yu_*/\nu. \tag{4.96}$$

The following classification of the inner region, which is based on experimental investigations, is commonly used.

(1) Viscous sub-layer $0 < y^+ < 5$.
(2) Buffer sub-layer $5 < y^+ < 30$.
(3) Fully turbulent sub-layer $30 < y^+ < 400$ ($y/\delta = 0.1$–0.2).

The viscous and turbulent stresses, given as functions of the y^+ values, are shown in Figure 4.15. Note that the total shear stress is almost constant over the inner region and is approximately equal to τ_w. Thus, this region is often referred to as the constant-stress layer.

In many situations it is inevitable that the boundary layer becomes detached from the wall. Boundary layers tend to separate from walls when there is an increasing fluid pressure in the direction of the flow; this is known as an adverse pressure gradient. While adverse pressure gradients reduce the wall shear stress through decreasing the flow velocity close to the wall, separation is often associated with a large increase in drag. Turbulent boundary layers can prevent or delay separation, thereby reduce the drag significantly. Thus, numerous methods by which to avoid or delay separation by creating turbulent boundary layers have been invented. The dimples on a golf ball are a good

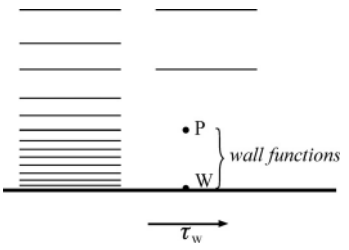

Figure 4.16 Application of wall functions to CFD simulation.

example of this. The interested reader can find more information about boundary-layer theory in [13].

4.3.2 Wall functions

Wall functions are empirical rules that are based on the logarithmic law of the wall. The wall functions may be needed in order to avoid having dense meshes in CFD simulations or they may be needed since particular turbulence models are not valid in the viscosity-affected near-wall region. The wall functions estimate the velocities $\langle U_i \rangle$, k and ε or $\langle u_i u_j \rangle$ in the RANS models in the first cell close to the wall. A wall function is also used for estimation of temperature, T, and concentration, C, in heat- and mass-transfer simulations.

Standard wall functions

The basic idea of the wall-function approach is to apply boundary conditions some distance away from the wall so that the turbulence model is not solved close to the wall. The wall functions allow calculations to be carried out with the first grid point, P, in the region where the wall function is valid, rather than on the wall itself, as shown in Figure 4.16. The boundary conditions are used at P, which represents the first grid point, and W represents the corresponding point on the wall. Thus, the wall functions allow the rapid variations of flow variables that occur within the near-wall region to be accounted for without resolving the viscous near-wall region.

In addition, the use of wall functions obviates the need to modify the turbulence models to account for the viscosity-affected near-wall regions. The mean velocity in the inner region of the boundary layer can be formulated in the universal form

$$\langle U \rangle^+ = f\left(y^+\right). \tag{4.97}$$

Assuming that the total stress τ_w is constant and the turbulent part of the total stress tensor is negligible in the viscous sub-layer, Eq. (4.91) reduces to

$$\frac{\tau_w}{\rho} = \nu \frac{\mathrm{d}\langle U_x \rangle}{\mathrm{d}y}. \tag{4.98}$$

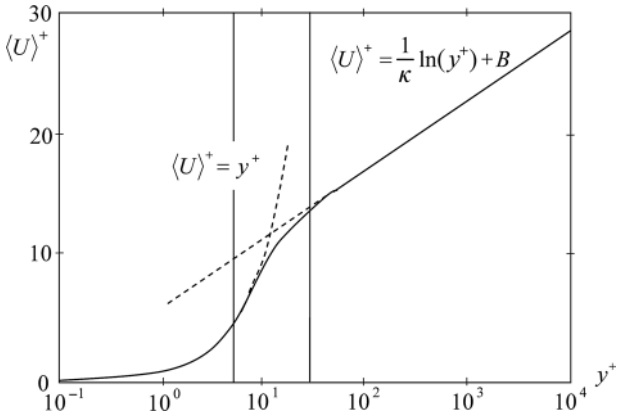

Figure 4.17 The law of the wall.

Integrating with respect to y and applying the no-slip boundary condition gives

$$\langle U_x\rangle = \frac{\tau_w y}{\rho \nu} = \frac{u_*^2 y}{\nu} \tag{4.99}$$

or in dimensionless form

$$\langle U_x\rangle^+ = y^+. \tag{4.100}$$

In the fully turbulent layer, the total stress tensor reduces to $\tau_{xy} = -\rho\langle u_x u_y\rangle$. Since the shear stress is almost constant over the inner region of the boundary layer and is approximately equal to τ_w, we obtain

$$\tau_w = -\rho\langle u_x u_y\rangle. \tag{4.101}$$

By introducing Prandtl's mixing-length model and the relation $l = \kappa y$, we obtain

$$\frac{\tau_w}{\rho} = -\langle u_x u_y\rangle = l^2\left(\frac{\mathrm{d}\langle U_x\rangle}{\mathrm{d}y}\right)^2 = \kappa^2 y^2\left(\frac{\mathrm{d}\langle U_x\rangle}{\mathrm{d}y}\right)^2. \tag{4.102}$$

Recall that the characteristic velocity scale for the sub-layers is given by $u_* = \sqrt{\tau_w/\rho}$. Equation (4.102) can now be written as

$$u_*^2 = \kappa^2 y^2\left(\frac{\mathrm{d}\langle U_x\rangle}{\mathrm{d}y}\right)^2. \tag{4.103}$$

On taking the square root of both sides and integrating with respect to y, we obtain the logarithmic velocity profile, which in dimensionless form reads

$$\langle U_x\rangle^+ = \frac{1}{\kappa}\ln\left(y^+\right) + B, \tag{4.104}$$

where $\kappa \approx 0.42$ and $B \approx 5.0$ (κ is the von Kármán constant). Equation (4.104) is referred to as the logarithmic law of the wall or simply the log law. Thus, in the viscous sub-layer the velocity varies linearly with y^+, whereas in the buffer sub-layer it approaches the log law, as shown in Figure 4.17.

Besides the logarithmic profile for the mean velocity, the wall functions also consist of equations for the near-wall turbulence quantities. There is no transport of k to the wall, while ε often has a maximum at the wall, but the derivation of the boundary conditions for the turbulence quantities is beyond the scope of this book. Note that, in the derivation of the boundary conditions for the turbulence quantities, it is assumed that the flow is in local equilibrium, which means that production equals dissipation. The boundary condition for k is given by

$$k = \frac{u_*^2}{C_\mu^{1/2}} \tag{4.105}$$

and that for ε by

$$\varepsilon = \frac{u_*^3}{\kappa y}. \tag{4.106}$$

The use of wall functions requires that the first grid point adjacent to the wall is within the logarithmic region. Ideally, the first grid point should be placed as close to the lower bound of the log-law region as possible in order to get as many grid points in the boundary layer as possible. In terms of dimensionless distance, that is $30 < y^+ < 100$. The wall-function approach saves considerable computational resources because the viscosity-affected near-wall region does not need to be resolved. The log law has proven very effective as a universal function for the inner region of the flat-plate turbulent boundary layer and it has been verified experimentally in numerous studies. Wall functions can successfully be used in many CFD simulations, and most CFD programs adjust the wall function accordingly when $y^+ < 30$, but $y^+ > 300$ should be avoided. However, doubts can be raised about the validity of wall functions under conditions such as strong pressure gradients and separated and impinging flows. Under such conditions the quality of the predictions is likely to be compromised. This does not mean that such flows cannot be simulated, rather that standard wall functions are not an appropriate choice. In the following sections we will introduce non-equilibrium wall functions and also a near-wall modelling approach whereby the viscous sub-layer actually is resolved.

Wall functions for non-equilibrium turbulent boundary layers

Non-equilibrium turbulent boundary layers are boundary layers that have been perturbed from the normal flat-plate boundary-layer state. Recall that the log law for the normal flat-plate boundary layer was derived under the assumption of constant shear. A local equilibrium between production and dissipation was also assumed in the derivation of the turbulence quantities. Thus, difficulties arise in applying standard wall functions when the simplifying assumptions upon which the wall functions are based are not applicable. Constant shear and the local-equilibrium hypothesis are therefore the conditions that most restrict the universality of the standard wall functions. In a boundary layer experiencing an adverse pressure gradient, the fluid closest to the wall is retarded due to the pressure increase in the streamwise direction. As a result, the wall shear stress is decreased. Consequently, adverse pressure gradients alter the mean velocity profile as

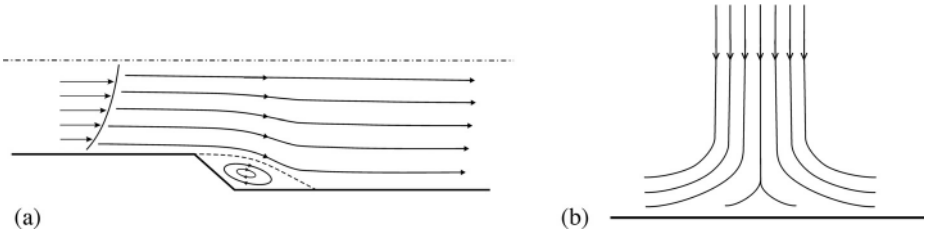

Figure 4.18 (a) Flow separation with a recirculation zone and a reattachment point. (b) Impinging flow.

well as the turbulence in the boundary layer. This means that, when the pressure gradient is strong enough, the logarithmic boundary-layer representation (the log law) cannot be used. Hence, for several flow conditions, e.g. flow separation and reattachment, strong pressure gradients and flow impinging on a wall (Figure 4.18), the flow situation departs significantly from the ideal conditions and the accuracy of the standard wall functions is low.

Modified wall functions that are capable to some extent of accounting for the effects of pressure gradients and departure from equilibrium have been developed. By using such modified wall functions for non-equilibrium boundary layers, improved predictions can be obtained. These wall functions typically consist of a log law for the mean velocity, which is sensitized to pressure-gradient effects. Boundary conditions for the turbulence quantities are derived using methods whereby the equilibrium condition is relaxed. Thus, these modifications further extend the applicability of the wall-function approach and allow improvements to be obtained for complex flow conditions.

4.3.3 Improved near-wall modelling

Improved modelling of wall-bounded flows can be achieved using a two-layer zonal approach or using low-Reynolds-number turbulence models. These techniques permit the governing equations to be solved all the way to the wall, thereby eliminating the use of wall functions and hence improving the wall shear-stress and wall heat-transfer predictions. Obviously resolution of the near-wall region including the viscous sub-layer requires a very fine near-wall grid resolution. Hence, this modelling approach requires a large amount of computational power compared with the wall-function approach.

Two-layer zonal modelling

In the two-layer zonal approach, the domain is divided into two zones or regions, as the name implies. These two regions may be identified by the wall-distance-based Reynolds number

$$Re_y = y\frac{\sqrt{k}}{\nu}, \tag{4.107}$$

where y is the distance to the nearest wall.

The fully turbulent region is normally taken to have $Re_y > 200$ and the viscosity affected region to have $Re_y < 200$. In the viscosity-affected near-wall region, a one-equation turbulence model for the turbulent kinetic energy is applied and an algebraic relation is used to determine the energy-dissipation rate. In contrast, a two-equation model such as the standard or more advanced k–ε model is employed in the fully turbulent region. Thus, in the viscous zone the energy dissipation is calculated from

$$\varepsilon = \frac{k^{3/2}}{l_\varepsilon}, \tag{4.108}$$

where l_ε is an appropriate length scale.

It is common practice to use a blending function to calculate the turbulent viscosity in the transition region. This function simply blends the turbulent viscosity in the viscosity-affected region with the turbulent viscosity in the turbulent region to obtain a smooth transition. Thus the blending function is defined as unity far from the wall and zero at the wall. The two-layer zonal approach requires approximately the same boundary-layer resolution as in the low-Reynolds-number approach. Since the energy dissipation is calculated from an algebraic equation, this approach may be more stable than the low-Reynolds-number approach.

Low-Reynolds-number turbulence models

One way of characterizing turbulence models is to distinguish between high- and low-Reynolds-number models. In the former, wall functions are used to approximate turbulence quantities close to walls. The standard k–ε model is an example of a high-Reynolds-number model. Whereas high-Reynolds-number models are valid for turbulent core flows, they are not valid in regions close to walls, where viscous effects predominate over turbulent ones. Low-Reynolds-number models are examples of models that are valid also in the viscous wall region and can thus be integrated all the way to the wall.

The low-Reynolds-number modifications typically consist of damping functions for the source terms in the transport equation for ε and in the expression for the turbulent viscosity. These modifications allow the equations to be integrated through the turbulent boundary layer, including the viscous sub-layer, thereby giving better predictions for near-wall flows. It is important to point out that these models are applicable for flows with high global Reynolds number wherein the flow is fully turbulent. These models are not useful for solving flows with low global Reynolds numbers. For that a transition model is needed. It should also be noted that these models are of ad-hoc nature and cannot be relied upon to give consistently good results for all types of flows. Low-Reynolds-number variants of the k–ε model include the Launder–Sharma and Lam–Bremhorst models.

For low-Reynolds-number models, the general transport equations for k are given by

$$\frac{\partial k}{\partial t} + \langle U_j \rangle \frac{\partial k}{\partial x_j} = \frac{\partial}{\partial x_j}\left(\left(\nu + \frac{\nu_\mathrm{T}}{\sigma_k}\right)\frac{\partial k}{\partial x_j}\right) + \nu_\mathrm{T}\left[\left(\frac{\partial \langle U_i \rangle}{\partial x_j} + \frac{\partial \langle U_j \rangle}{\partial x_i}\right)\frac{\partial \langle U_i \rangle}{\partial x_j}\right] - \varepsilon \tag{4.109}$$

and the general transport equations for ε are given by

$$\frac{\partial \tilde{\varepsilon}}{\partial t} + \langle U_j \rangle \frac{\partial \tilde{\varepsilon}}{\partial x_j} = \frac{\partial}{\partial x_j}\left(\left(\nu + \frac{\nu_\mathrm{T}}{\sigma_\varepsilon}\right)\frac{\partial \tilde{\varepsilon}}{\partial x_j}\right) + C_{1\varepsilon} f_1 \nu_\mathrm{T} \frac{\tilde{\varepsilon}}{k}\left[\left(\frac{\partial \langle U_i \rangle}{\partial x_j} + \frac{\partial \langle U_j \rangle}{\partial x_i}\right)\frac{\partial \langle U_i \rangle}{\partial x_j}\right] - C_{2\varepsilon} f_2 \frac{\tilde{\varepsilon}^2}{k} + E, \tag{4.110}$$

where the turbulent viscosity is calculated from

$$\nu_\mathrm{T} = f_\mu C_\mu \frac{k^2}{\tilde{\varepsilon}} \tag{4.111}$$

and the energy dissipation, ε, is related to $\tilde{\varepsilon}$ by

$$\varepsilon = \varepsilon_0 + \tilde{\varepsilon}. \tag{4.112}$$

The quantities ε_0 and E are defined differently for each model; ε_0 is the value of ε at the wall. The difference between these models and the standard k–ε model is the damping functions f_1 and f_2 in the transport equation of ε and the damping function f_μ. The damping functions are generally written in terms of specifically defined Reynolds numbers

$$Re_\mathrm{t} = \frac{k^2}{\nu\varepsilon} \tag{4.113}$$

and

$$Re_y = \frac{\sqrt{k}y}{\nu}. \tag{4.114}$$

Obviously the global Reynolds number has nothing to do with the low-Reynolds-number turbulence models. The low Reynolds number comes from the local Reynolds number.

4.3.4 Comparison of three near-wall modelling approaches

As has already been pointed out, the near-wall treatment determines the accuracy of the wall stresses and of the near-wall turbulence prediction. Hence, appropriate near-wall turbulence modelling is crucial in order to capture important flow features such as flow separation, reattachment and heat- and mass-transfer rates. Figure 4.19 illustrates the implementation of the three near-wall treatment approaches mentioned in the previous sections.

The general recommendation for a standard wall function is $30 < y^+ < 100$, preferably in the lower region. At high Re the log law is valid up to higher y^+ and the upper limit may increase to 300–500. For low-Re models and enhanced wall functions the first grid point should be close to $y^+ = 1$, and there should be at least ten grid points in the viscosity-affected near-wall region, i.e. $y^+ < 20$.

The lengths corresponding to $y^+ = 1$ and $y^+ = 30$ for pipe flows at various Reynolds numbers are given in Table 4.5 to give a feeling for the actual dimensions.

Table 4.5 Physical lengths corresponding to y^+ for flow through a smooth pipe, as a function of the Reynolds number

Re	$y^+ = 1$	$y^+ = 30$
5000	145 μm	4.4 mm
50 000	20 μm	0.60 mm
500 000	2.5 μm	0.075 mm
5 000 000	0.30 μm	0.0090 mm

Table 4.6 A summary of near-wall modelling approaches

Modelling approach	Physics	Grid requirements	Numerics
Wall functions	−	+	+
Low-Reynolds-number modifications	+/−	−	+/−
Zonal modelling	+/−	−	+

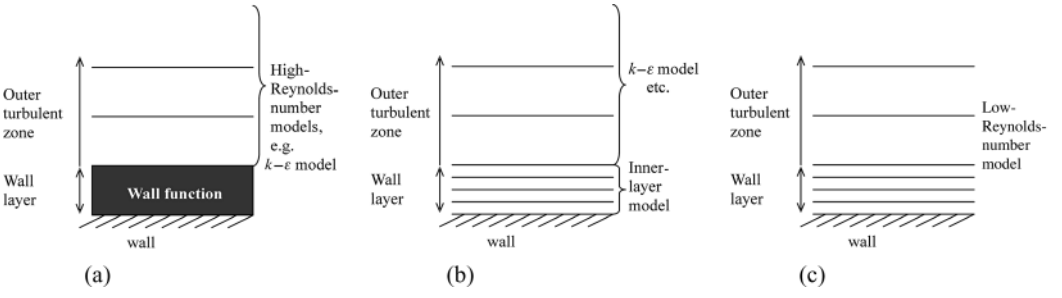

Figure 4.19 Illustrations of various near-wall treatment approaches: (a) the wall function; (b) the two-layer zonal approach; (c) low-Reynolds-number modifications.

It might not always be apparent what near-wall modelling approach to use in a certain simulation. As with the choice of selecting an appropriate turbulence model, the choice among the near-wall modelling approaches is strongly coupled to the physics of the particular flow and the computational resources available. The general pros and cons of the three approaches illustrated in Figure 4.19 are summarized in Table 4.6. This table indicates the level of physics involved, the computational power required and the numerical difficulties involved in implementing the three near-wall modelling approaches in CFD simulations.

4.4 Inlet and outlet boundary conditions

Simulation of turbulent flows requires knowledge of the turbulent quantities at all boundaries where the flow enters the computational domain. For a two-equation

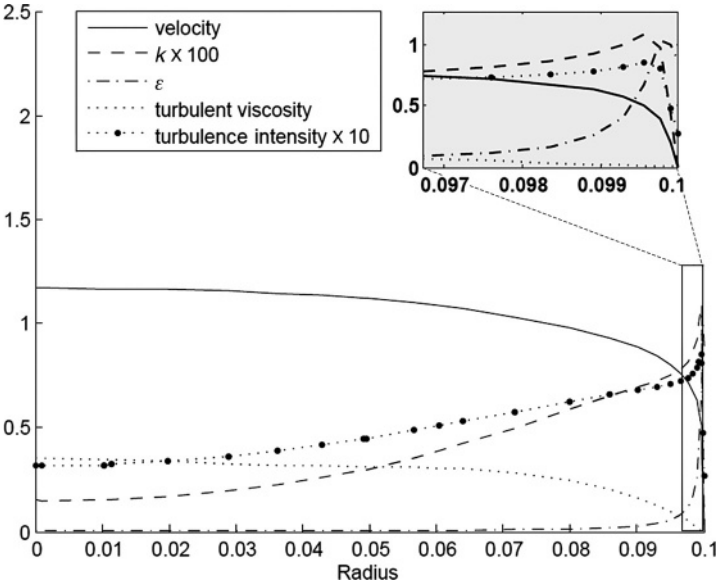

Figure 4.20 Velocity and turbulence properties in a cross-section of a pipe at $Re = 200\,000$.

turbulence model, such as the k–ε model, both the turbulent kinetic energy and the energy-dissipation rate should be specified. However, since it is the specification of the turbulence timescales, velocity scales and length scales entering the domain that defines the turbulence, it need not necessarily be the values of the turbulent kinetic energy and its dissipation rate that are specified. Instead of specifying these values, the boundary conditions are often specified in terms of the turbulence intensity, which is defined by the ratio of the fluctuating component of the velocity to the mean velocity, and a characteristic turbulence length scale. For internal flows, a turbulence intensity of 5%–10% and a length scale of 1%–10% of the hydraulic diameter are usually appropriate. Specifying boundary conditions for the Reynolds stress transport model is more difficult than for two-equation models, since all the stresses must be specified. If these are not available turbulence could be assumed to be isotropic at the inlet, i.e. zero shear stresses and the normal stresses given by $\frac{2}{3}k$. Always select boundary conditions with care since inconsistent boundary conditions may cause unrealistic reduction of the turbulence after the inlet, or turbulence may flow through the entire domain without changing.

Velocity and turbulence are usually not constant at the inlet and outlet, but depend both on upstream and on downstream conditions. The inlet and outlet should be located as far away from the region of interest as possible so that the approximations under the given conditions will not affect the results of the simulations. Figure 4.20 shows the radial variation of velocity and turbulence properties in a pipe at $Re = 200\,000$. Using the average properties for velocity, i.e. $U = 1$ m s^{-1}, is reasonable but k and ε have large radial variation and average values will not describe the actual inlet conditions. A better approximation is to use the turbulence intensity and turbulence length scale.

The turbulence intensity for a pipe at high Reynolds number can be estimated from

$$I = \frac{u}{\langle U \rangle} = 0.16 Re^{-1/8} \tag{4.115}$$

and the turbulence length scale is given by

$$l = 0.07L, \tag{4.116}$$

where L is the hydraulic diameter and $\overline{U}$ the average velocity. It is then possible to estimate k and ε from

$$k = \frac{3}{2}(\langle U \rangle)^2 \qquad \text{and} \qquad \varepsilon = C_\mu^{3/4} \frac{k^{3/2}}{l}. \tag{4.117}$$

4.5 Summary

Turbulence is of considerable importance in most flows of engineering interest, so turbulence modelling is one of the key elements to successful CFD simulations. In this chapter the physical and mathematical principles underlying turbulence modelling were explained. The purpose of this chapter was, besides providing a survey of turbulence models, also to indicate their validity and limitations in various applications. Even though we have far from exhausted all aspects, this chapter serves as an overview of turbulence modelling. Readers who are particularly interested in turbulence modelling are encouraged to turn their attention to the references given in this book for more in-depth discussions of this subject.

Questions

(1) Discuss why turbulence has to be modelled.
(2) Explain the origin of the Reynolds stresses in the RANS equations and explain what is meant by the closure problem.
(3) Explain what is meant by the Boussinesq approximation.
(4) What limitations does the Boussinesq approximation impose on a turbulence model?
(5) Discuss the application of zero-, one- and two-equation models.
(6) Discuss the differences between Reynolds stress modelling and eddy-viscosity-based modelling.
(7) Explain what is meant by large-eddy simulations.
(8) Explain what is meant by wall functions, why they are used and when it is appropriate to use them.
(9) Discuss how the near-wall treatment can be improved, i.e. when the wall-function approach is not appropriate.
(10) Discuss what turbulence boundary conditions it is appropriate to use.